

Performance characterization of shielded metal arc welding power supply designs

By

Rangarajan Padmanabhan

A thesis presented
to the University of Waterloo
in fulfilment of the
thesis requirement for the degree of
Master of Applied Science
in
Mechanical and Mechatronics Engineering

Waterloo, Ontario, Canada, 2019

© Rangarajan Padmanabhan 2019

Author's Declaration

I hereby declare that I am the sole author of this thesis. This is a true copy of the thesis, including any required final revisions as accepted by my examiners.

I understand that my thesis may be made electronically available to the public.

Abstract

Engine driven welding power supplies are widely used for Shielded metal arc welding process in field applications such as pipeline industry, where there is a lack of electricity grid. Being a manual process, the welder's preference towards a DC generator based power supply over a chopper based power supply requires the need for scientific/quantitative evidence to back the reasons for this preference. Due to differences in the mechanism used to control the current, the current pulse profile generated by either machine is different from one another. This difference in the current profile affects the metal transfer phenomenon as well as the arc stability causing difficulty to the welder. Therefore, current and voltage signals collected using high-speed data acquisition system was analyzed and these signals were synchronized with high-speed video in order to observe and explain the mode of metal transfer. The experiments were performed with operators of different experience levels; at different welding positions in order to determine how the characteristic of power supply alone truly affect the current, voltage signals and metal transfer. Auxiliary outputs such as melt-off rates, and the ease of bridging increasing gaps were used for further comparisons between the power supplies. The results showed the predominant mode of metal transfer for either electrodes, E6010 and E7018. Results from heatscatter plots and high-speed videos explain the reasons provided by the welders for their preference towards DC generator based power supply. Lower voltage range provided by the DC generator based power supply explains for the tighter arc produced by it, while the higher current range and rapid arc movement at the tip of the electrode explains the easier arc control and restart-ability provided by the DC generator based power supply. Moreover, at the same average current level for both power supplies, DC generator based power supply produced a better melt-off rate compared to chopper based power supply, affecting the productivity.

Acknowledgements

First of all, I owe my gratitude to my supervisor, well-wisher and the most humane person I have come across in my life, Prof. Adrian P. Gerlich. Thank you for providing me with an opportunity to do my internship, Masters studies, my first TA experience etc. There was not one point in my masters, where I felt overwhelmed because of you. Thanks for your support and guidance, right from the day I met you (May 11, 2015) which I hope will be there for the rest of my life. I am really grateful for all the opportunities that resulted because of your help.

Secondly, I would like to thank MITACS Canada for organizing and funding my internship, which served as the reason for my perusal of masters.

My masters studies or this thesis would not be complete without my gratitude for all the CAMJ members, Abdelbaset Midawi, Emanuel Dos Santos, James Choi, Luqman Shah, Nazmul Huda, Rafael Ribeiro, Rahul Ram and Soheil Bakhshivash. Thank you being there whenever I have need support and guidance with research work as well as the personal matters. I have enjoyed the conversations I have had with each of you.

Huge thanks to Rob Kraemer from the Engineering machine shop for training me in stick welding, as well as his timely help in performing the experiments as the experienced welder.

I, also thank Prof. Peter Balka for providing me with the opportunity to assist him in teaching an undergraduate course which has helped me develop my teaching skills and presentation skills.

Finally, I owe a lot to my mother and father for their unconditional love and support.

Table of Contents

List of Figures	vii
1 Introduction	1
1.1 Motivation - - - - -	3
1.2 Objective - - - - -	4
1.2.1 Main objective - - - - -	4
1.2.2 Specific Tasks Required - - - - -	4
2 Literature Review	5
2.1 Shielded Metal Arc Welding (SMAW) - - - - -	5
2.2 Arc Sources - - - - -	7
2.3 Electrodes and metal transfer modes - - - - -	11
2.4 Welding power supplies - - - - -	15
3 Experimental Parameters	20
3.1 Welding parameters - - - - -	20
3.2 High-speed Imaging - - - - -	23
4 Results and Discussions	26
4.1 Voltage and Current Oscillograms and Histograms - - - - -	26
4.2 Heatscatter (Voltage/Ampere) Plots - - - - -	33
4.3 High Speed Imaging - - - - -	38
4.4 Auxiliary Output Comparisons - - - - -	43
4.5 Explanations for the reasons provided for the preference - - - - -	51

5 Concluding remarks and recommendations for future work 53

5.1 Conclusions ----- 53

5.2 Recommendations for future work ----- 55

References 56

Appendix A 59

List of Figures

Figure 1-1:	Welding of cover pass on a joint in Industrial Piping using SMAW [4]	1
Figure 1-2:	SMAW is widely used for Maintenance and Repair [4]	2
Figure 2-1:	Shielded metal arc welding process [14]	6
Figure 2-2:	Output curves for CC and CV Power sources [16]	8
Figure 2-3:	Effect of arc voltage on arc length [16]	9
Figure 2-4:	Arc voltage distribution with respect to arc length [17]	10
Figure 2-5:	Standard Voltage/Ampere Curve for CC power source [18]	11
Figure 2-6:	Electrode classification according to AWS standards [19].....	12
Figure 2-7:	Pictorial depictions of transfer modes observed in SMAW [20]	13
Figure 2-8:	Different modes of metal transfer that take place in E6010 electrode [22]	14
Figure 2-9:	Short circuit metal transfer in E7018 electrode [22].....	14
Figure 2-10:	a) PDD of voltage signals of E6010; b) PDD of voltage signals of E7018 [24]....	15
Figure 2-11:	Internal structure of DC generator Classic 300MP [25]	16
Figure 2-12:	Internal components of Solid-state BigBlue 350 PipePro [28].....	18
Figure 2-13:	Current waveform during short circuit observed when using (a) DC generator; (b) Solid-state.....	18
Figure 2-14:	Current and Voltage Oscillograms when welded using (a) DC generator based power supply; (b) Inverter based power supply [24]	19
Figure 3-1:	Fixture used to replicate pipeline welding.	22

Figure 3-2:	Arc appearance for aperture f/22 using 515 nm wavelength band pass filter for different exposure times [29].	24
Figure 3-3:	Arc appearance for aperture f/22 using 900 nm wavelength band pass filter for different exposure times [29].	25
Figure 4-1:	Voltage and Current Oscillograms generated during welding with E7018 electrode by an inexperienced operator, using (a) DC generator (b) Solid-state welder.	27
Figure 4-2:	Voltage and Current Oscillograms generated during welding of E6010 by an inexperienced operator.	28
Figure 4-3:	Current waveform during short circuit with (a) DC generator, (b) Solid-state.	29
Figure 4-4:	Current derivative plots when welding was performed with (a) DC generator, (b) Solid-state.	30
Figure 4-5:	Histograms generated with current signals when welding was performed with (a) DC generator, (b) Solid-state by an inexperienced operator.	31
Figure 4-6:	Effect of Inductance on current during short circuit event [30].	31
Figure 4-7:	Voltage and Current Oscillograms generated during welding of E7018 using (a) DC generator: (b) Solid-state by an experienced operator	32
Figure 4-8:	Voltage and Current Oscillograms generated during welding of E6010 using (a) DC generator: (b) Solid-state by an experienced operator.	33
Figure 4-9:	Heatscatter plots generated from current and voltage signals, when welding was performed with E7018 by an inexperienced operator using (a) DC generator, (b) Solid-state power supply	34
Figure 4-10:	Heatscatter plots generated from current and voltage signals, when welding was performed with E7018 by an experienced operator using (a) DC generator, (b) Solid-state power supply	34
Figure 4-11:	Heatscatter plots for welding performed at 45° downhill with E6010 using (a) DC generator, (b) Solid-state power supply	36
Figure 4-12:	Heatscatter plots for welding performed at 45° downhill position with E7018 using (a) DC generator, (b) Solid-state	36

Figure 4-13: Heatscatter plots for welding performed at downhill position with E8010 using (a) DC generator, (b) Solid-state.	37
Figure 4-14: Region of concentrated points approximated to ellipse when welded using (a) DC generator, (b) Solid-state	38
Figure 4-15: High-speed images synchronized with current and voltage signals to explain a short circuit transfer.	39
Figure 4-16: Series of high speed images during a short circuit event; Solid-state power supply, E6010 and Inexperienced operator.....	40
Figure 4-17: Series of high speed images to explain the flux-wall guided metal transfer; Solid-state power supply, E7018 and inexperienced operator.....	41
Figure 4-18: High-speed images recorded with 515nm lens for E7018 using DC generator power supply.	42
Figure 4-19: High-speed images recorded with 515nm lens for E7018 using Solid-state power supply.	42
Figure 4-20: Illustration of arc movement at the tip of the electrode E7018 using (a) DC generator, (b) Solid-state power supply.	43
Figure 4-21: Power plot using (a) DC generator power supply, (b) Solid-state power supply. .	45
Figure 4-22: Plot of acceleration vs time for both power supplies.	45
Figure 4-23: Plot of acceleration derivative vs time using (a) DC generator, (b) Solid-state. ...	46
Figure 4-24: X-Ray of samples of increasing gap welded using (a) DC generator power supply (b) Solid-state power supply.	47
Figure 4-25: Comparison of melting rates of E6010 between power supplies; operator (a) Experienced, (b) Intermediate, (c) Novice.....	47
Figure 4-26: Comparison of melting rates of E7018 between power supplies; operator (a) Experienced, (b) Intermediate, (c) Novice.	48
Figure 4-27: Bead appearance for welds performed at 45° downhill position by an experienced pipeline welder using (a) DC generator power supply, (b) Solid-state power supply.	50

Figure 4-28: Heatscatter plots generated from voltage and current signals recorded when using Solid-state power supply with (a) Low AFC, (b) High AFC. 51

Chapter 1

Introduction

Shielded Metal Arc Welding (SMAW), also known as Manual Metal Arc Welding (MMAW) or informally as stick welding, is one of the oldest, most widely used, and versatile welding processes. SMAW is best for making strong welds on metals that is not clean enough to be welded with other processes like GMAW [1] and was the predominant form of fusion welding until the 1980's [2]. It also has the advantage of not requiring a shielding gas, and can even be performed under water due to the weld pool being self-shielded by the decomposing electrode coating. The applications of SMAW encompasses a wide variety including pressure vessels, industrial piping, ships, transportation, repair and maintenance industry etc. Owing to the equipment's portability and ease of operation, SMAW can be performed at a distance from the power source, which makes it the ideal choice for welding in the field (off-grid) [3]. Presently, with various other modern welding processes, SMAW's application has been limited to the field of pipeline welding and in the repair and maintenance industry [4]. Figures 1-1 and 1-2 show the application of SMAW in industrial piping and maintenance repair industry respectively.



Figure 1-1: Welding of cover pass on a joint in Industrial Piping using SMAW [4]

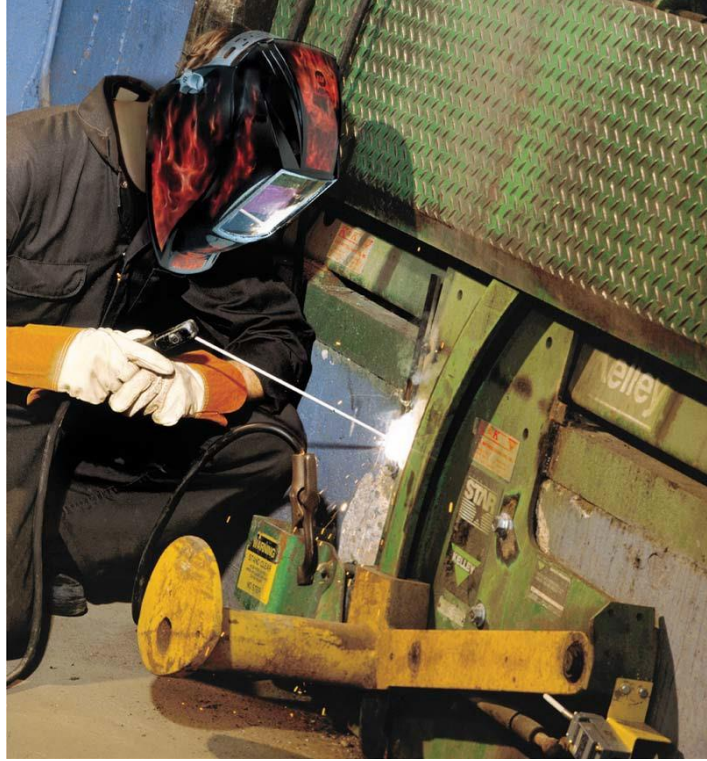


Figure 1-2: SMAW is widely used for Maintenance and Repair [4]

The power supplies that are used for SMAW are available in different designs, commonly referred to as Transformer; Generator or Alternator; and Inverter-based solid state designs [5]. These power supply designs are different in the way they produce and control the current required for the welding process. Transformer and Inverter based power supplies are connected to the facility mains (230 or 115 VAC) directly to generate AC, which is then converted to DC with the use of a rectifier. On the other hand, Generator and Alternator based power supplies locally convert mechanical energy into electrical energy and therefore, use internal combustion engines or an electric motor to drive the generator or alternator. In the case of a generator, Direct Current is produced where as an alternator produces an AC, which is rectified to DC. The power supplies under the present study come under the second category of the design type, which use diesel engines to produce current and therefore, can be used in field applications where the electricity grid is not available. The differences will be investigated between a DC generator based power

supply [6] and a solid-state power supply [7] that uses an alternator to generate the electrical energy. Since these power supplies differ in the way they control the current during the welding process, the current pulse profile generated by the machines is different. The DC generator based power supply control the current by tapping different combinations of windings inside the generator while chopper based power supply uses the chopper circuit to control the current, and this can lead to inherent differences in the weld output and welder experience.

1.1 Motivation

A survey was conducted among the pipeline welders about their preference for the type of power supply, given the two designs, DC generator based and solid-state based [8]. Most welders exhibit a preference was towards DC generator based power supply for the following reasons:

- DC generator based power supply apparently provides a tighter arc
- DC generator based power supply provides an arc that is easier to control
- Easy restart-ability of the arc with DC generator based power supply. Easy restart-ability would mean it is relatively easier to break the arc, cool the electrode and restart the arc.

A question remains regarding whether these reasons are due to the difference in metal transfer phenomenon or other inherent characteristics of the power supply. Are the above reasons a result of the difference in the profile of the current pulse generated by the two power supplies? There is little scientific or quantitative evidence to back the claims above. Therefore, the primary motivation is to explain the reasons for this preference. Moreover, solid-state power supplies have a few advantages over the DC generator based power supply, such as low cost, higher efficiency and lower maintenance. Another motivation is quantify the characteristics of the power supply

responsible for the desirable qualities mentioned, and try to incorporate those features into a solid state power supply which is less costly to manufacture.

1.2 Objective

1.2.1 Main Objective

The main objective of this study is to try to identify the key electrical characteristics of the DC generator based power supply that is responsible for producing a relatively stable arc that is preferred by the pipeline welders.

1.2.2 Specific Tasks Required

In order to achieve the main objective, the following specific objectives will be targeted:

- Record voltage and current signals throughout the welding time using a high-speed Data Acquisition (DAQ) system.
- Compare the Voltage/Ampere plots in order to find the effect of the power supply after cancelling out the effect of operator's influence, electrode and position of welding.
- Setup a high-speed camera and with the use of 900 nm and 515 nm wavelength filters, observe the molten pool and metal droplet formation and correlate the metal transfer phenomenon with current and voltage signals by synchronizing the DAQ system to the high-speed camera.
- Conduct additional tests to determine the melt-off rates, ease of gap bridge-ability etc. in order to find if either of the power supply electrical output is connected to higher welding productivity or lower cost.

Chapter 2

Literature Review

2.1 Shielded Metal Arc Welding (SMAW)

Shielded metal arc welding (SMAW) or Manual metal arc welding (MMAW) is a welding process in which an electric arc is produced, with either alternating current or direct current, between the metal plate and the electrode as shown in Fig. 2-1. The coating of the electrode disintegrates to form the shielding gas, as well as the slag on top of the molten metal for protection from surrounding atmospheric contamination [9]. In this process, the operator has to strike the electric arc by bringing the electrode in contact with the workpiece, gently touching it and slightly pulling the electrode of the plate. This gives the necessary contact to close the electric circuit, which in turn initiates the arc, thereby melting the consumable electrode and metal plate together.

Informally, SMAW is known as stick welding, and is one of the oldest welding processes, with its invention dating back to the last decade of the 19th century, when Nikolay Slavyanov [10] invented the consumable electrode. The patenting of carbon arc welding by Benardos and Olszewski in the year 1887 [11] preceded this. Coffin further developed this into an arc welding process in the year 1990, which consumed a metal electrode [12]. The difference between this process and the present-day SMAW is that coated electrodes are currently used for the welding process. Strohmenger released the first coated electrodes [13], and Kjellberg introduced electrode coatings in the 1900's which helped to stabilize the arc. Nowadays, electrodes are available in variety of different coatings and choice of a particular electrode will depend on specific requirements of the welding project. The detailed chemistry and designation systems used for coated electrodes will be discussed in the following section.

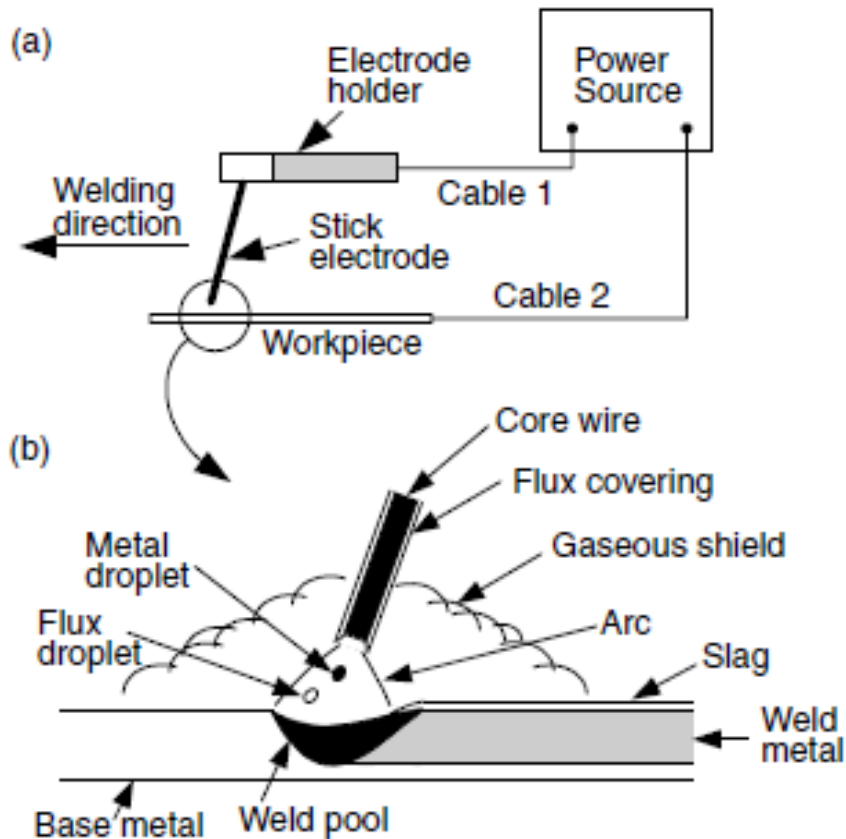


Figure 2-1: Shielded metal arc welding process [14]

The major advantage of SMAW process is that the equipment used for welding is inexpensive and portable, making it the preferred choice of welding in the maintenance and repair industry. The process is very flexible, considering welds can be made in any position that can be reached by an electrode and with the use of long leads, and welding can be performed in locations where it is difficult to use other welding equipment/processes. However, the major disadvantage of the process is the continuity. The operator has to stop the process after the entire electrode is consumed and replace the electrode. This in turn leads to a low duty cycle and overall lower deposition rates as compared to a continuously fed electrode process. Moreover, SMAW is not suitable for butt welds and larger fillet welds [15].

2.2 Arc Sources

Welding power supplies are characterized by two main electrical characteristics: current and voltage. However, most welding power supplies are capable of maintaining only one of them at a constant level, while the other variable is dependent on other factors involved in the welding process. Therefore, there are two types of arc control namely, constant current (CC) and constant voltage (CV) [16], and relationship between these determines the output curves based on the CC and CV setting as shown in Fig 2-2. On the left side of the figure, we have the constant current settings where the amount of change in voltage is large compared to the current. Even though the name suggests “constant current”, it is difficult for the welding power supply to maintain the current at an exact level because of the fact that the dynamic welding arc has a varying resistances so that the current (A) and voltage (V) changing constantly with various modes of metal transfer which includes short-circuit, spray projected, globular and explosive, which makes the term “constant” in this case relative. The power supply reacts every millisecond to the rapidly changing current and voltage and tries to maintain either of them at a constant level depending on which power source setting is selected. The effects of current and voltage on the welding process are important to understand as it explains the reason for preference of a particular power source for a particular welding project.

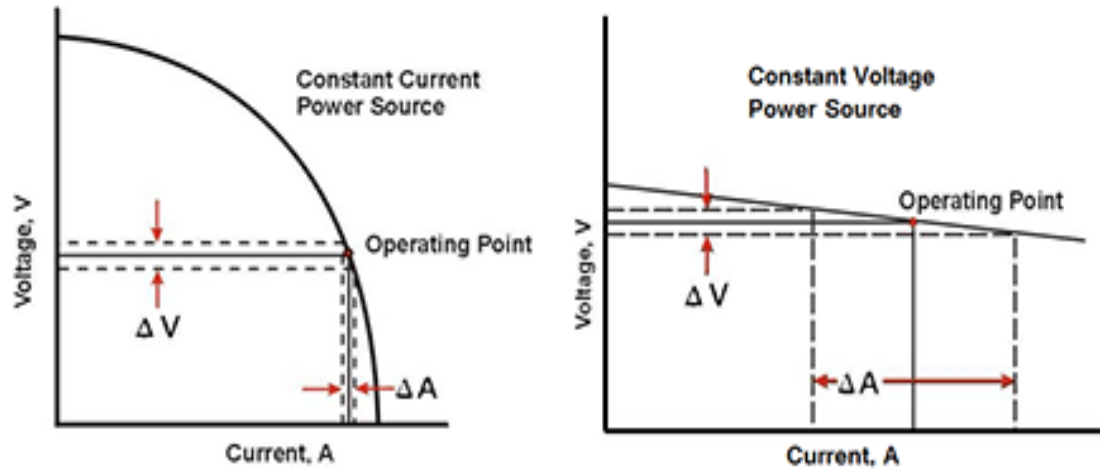


Figure 2-2: Output curves for CC and CV Power sources [16]

The response of the arc to changes in current and voltage will control the electrode consumption rate as well as the final bead appearance. Current is mainly responsible for controlling the melting rate of the consumable electrode, or the continuously fed wire in Gas Metal Arc Welding (GMAW), where increasing the current is directly related to higher melt-off, and decreasing the current will reduce the melt-off rate of the electrode. Voltage, on the other hand largely determines the arc length, which in turn controls the bead appearance and width. This occurs because as the arc length is increased or decreased, the resulting width and volume of the arc cone increases or decreases respectively. This is shown in the following figure, where arc length is defined as the distance between the metal workpiece and the tip of the electrode. Apart from current and voltage, the welding speed is also responsible for the final bead appearance. Given the same current and voltage setting, the higher the welding speed, the smaller is the width of the bead, and vice versa. The type of the power source used is dependent on the welding process for which it is used. In the case of manual processes like SMAW and Gas Tungsten Arc Welding (GTAW), where the operator is responsible for striking the arc and welding the plate, it is difficult

for the operator to maintain a constant arc length, which means it is difficult to maintain at a constant voltage.

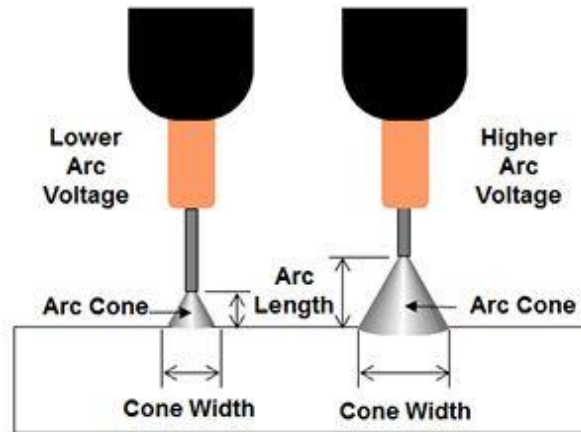


Figure 2-3: Effect of arc voltage on arc length [16]

Therefore, constant current (CC) is normally preferred for these welding processes where the current is maintained at a relatively constant level, allowing a wider voltage range that gives the operator the flexibility to weld with a constant melting rate across different arc lengths. On the other hand, with continuously wire-fed processes like GMAW or semi-automatic process like Flux Cored Arc Welding (FCAW), constant voltage (CV) power source is preferred. Since, it is a semi-automatic process where the speed of wire feeding system is controlled automatically; it is easier to maintain a constant arc length. This is because, as the wire feed speed is reduced, the distance between the wire and the plate is increased, which results in the reduction of the melting rate due to variation in the current level, which in turn will bring the arc length back to normal. If, on the other hand the speed of wire feeding system is increased to bring the wire is closer to the plate, there will be an increase in the melting rate, and once again the arc length will be brought back to normal length (referred to as self-sustaining arc).

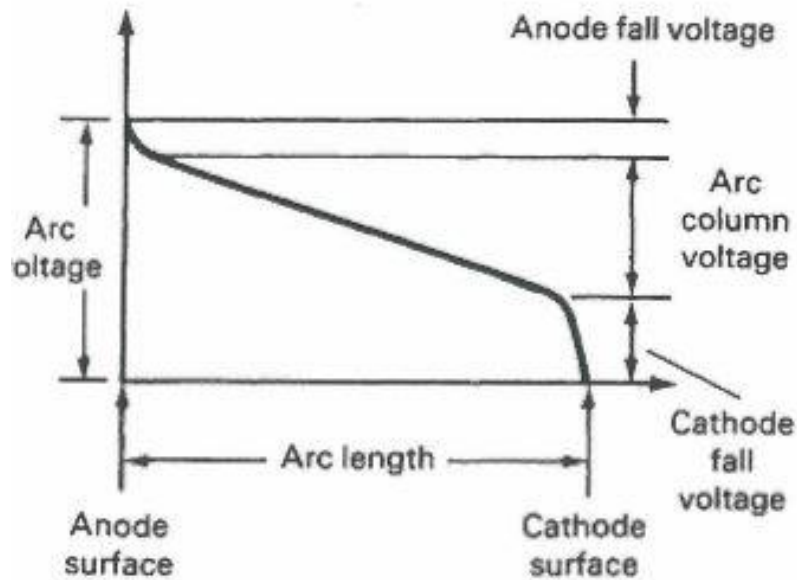


Figure 2-4: Arc voltage distribution with respect to arc length [17]

In terms of arc physics, the relationship between arc voltage and arc length can also be shown by the plot in Fig 2-4. Hoyaux et al. [17] discusses the three distinct regions observed in the welding arc: the cathode, the arc column and the anode. The flow of electrons from the cathode through the arc column to the anode forms the arc, which consists of metal droplets, flux constituents, electrons, ionized gasses, and metal vapour. It is worth noting that a characteristic constant current voltage vs. ampere plot is usually recorded for SMAW process. Considering the plot in Fig 2-5, SMAW max represents the peak value of the current surge when a short circuit happens in the welding process. Another important feature to note is the arc force control, which varies from 0% to 100%. The Arc Control shown in Fig 2-5 is sometimes denoted as Arc Force Control (AFC) as a variable accessible on some welding power supplies, which allows one to adjust the amount of limiting current in case of stick welding. This is directly related to the amount of current or heat that is generated under the short circuit conditions. Short circuit conditions arise when the voltage drops close to zero (with a minimum Short circuit voltage depending on the

electrode and lead lengths) and this can be observed in the plot. When the value of voltage tends to zero, there is surge in current value and the peak of this current value is determined by the arc force control, and the magnitude of this is sometimes referred to as ‘dig’ by welders. The voltage/ampere plot relationship is also known as the VI plot, which will be the characteristic used to differentiate the performance of the power supplies under study in this thesis.

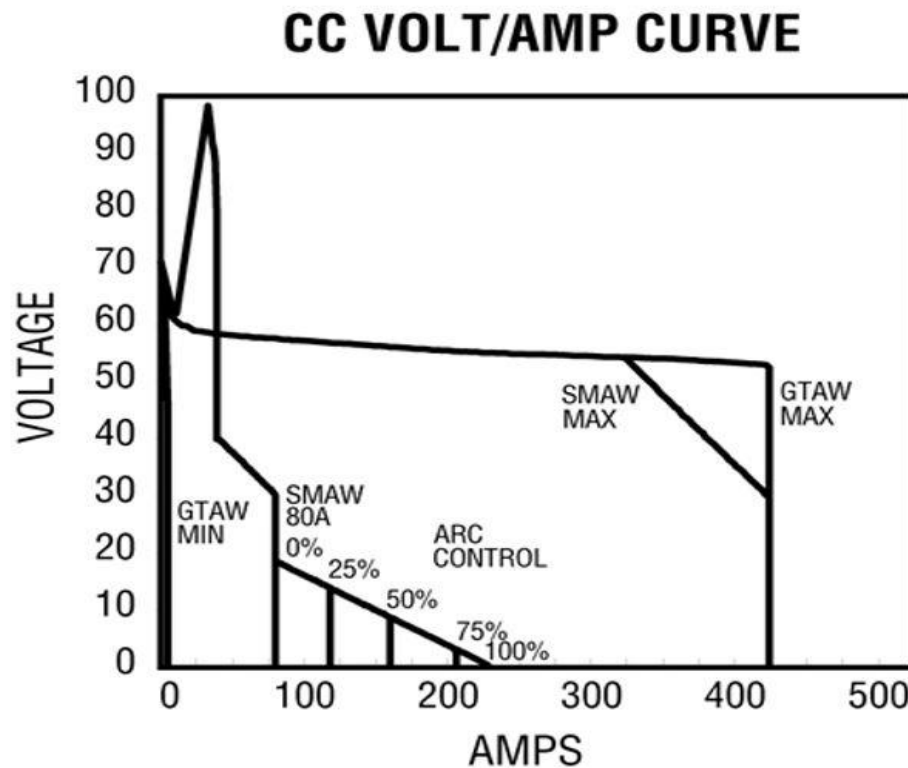


Figure 2-5: Standard Voltage/Ampere Curve for CC power source [18]

2.3 Electrodes and metal transfer modes

The electrodes used for the current study are E6010, E7018 and E8010. These electrodes are classified according to the AWS into a 4 or 5 digit number preceded by the letter E. The letter E denotes the electrode, and the first two digits of a four-digit number and first three digits of a five-digit number represent the minimum tensile strength of the welded metal in terms of

kilopound per square inch (ksi); for example, E60xx denotes that min. tensile strength is 60 ksi (414 MPa). The second last digit specifies the positions that can be welded with that particular electrode; for example, Exx1x denotes all position, Exx2x means that the electrodes can be used for only flat and horizontal position while Exx4x indicates an electrode that can be utilized for flat, vertical down, horizontal and overhead positions. Finally, the last digit represents the coating on the electrode along with a corresponding preferred polarity of the current, either DCEP, DCEN or AC. DCEP means Direct current with electrode as the positive terminal and DCEN means direct current with the electrode as the negative terminal. The classification system is summarized in Fig 2-6 while the type of coating and the preference of the current/polarity is given in the Table 2-1.



Figure 2-6: Electrode classification according to AWS standards [19]

Table 2-1: Chart showing type of coating/ welding current for the last digit

Digit	Type of Coating	Welding Current
0	High cellulose sodium	DC+
1	High cellulose potassium	AC, DC+ or DC-
2	High titania sodium	AC, DC-
3	High titania potassium	AC, DC+
4	Iron powder, titania	AC, DC+ or DC-
5	Low hydrogen sodium	DC+
6	Low hydrogen potassium	AC, DC+
7	High iron oxide, iron powder	AC, DC+ or DC-
8	Low hydrogen potassium, iron powder	AC, DC+ or DC-

The electrode E6010 can be used in all positions and provides an arc, which has a penetrating effect enabling it to dig through paint, rust, oil or dirt. This electrode's penetrating arc comes from the design of the electrode, so that it can be used for the root pass. E6010 does not provide a good final bead appearance and it is slightly difficult to remove the slag. On the other hand, E7018, also known as basic electrode, is made of low hydrogen potassium and iron powder and are predominantly used for the fill passes and produces a slag which is very easy to remove. Similar to E6010, this electrode can be used for all positions as well. Unlike E6010, which is very difficult to weld with for beginners, E7018 is relatively easier to weld for beginners.

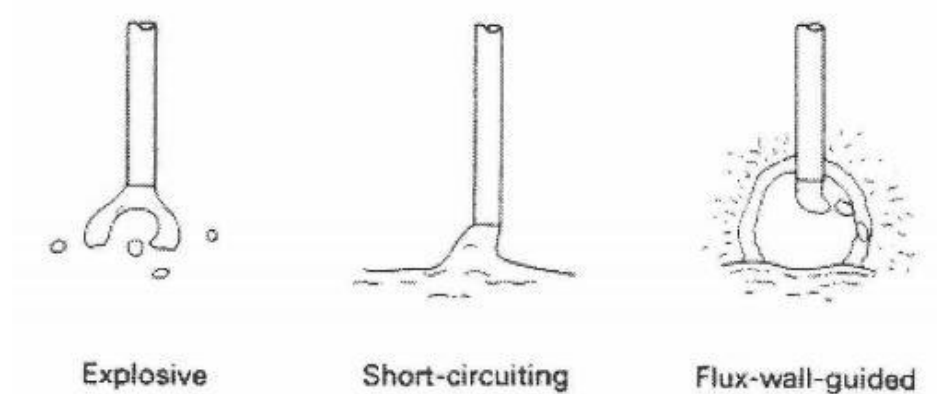


Figure 2-7: Pictorial depictions of transfer modes observed in SMAW [20]

In his work, Xu mentions that the metal transfer modes that are exhibited in the shielded metal arc welding process are primarily, short circuit transfer, flux-wall guided transfer and explosive transfer (the predominant mode of transfer in most conditions) [21] can be shown by the pictorial depictions in the Fig 2-7.

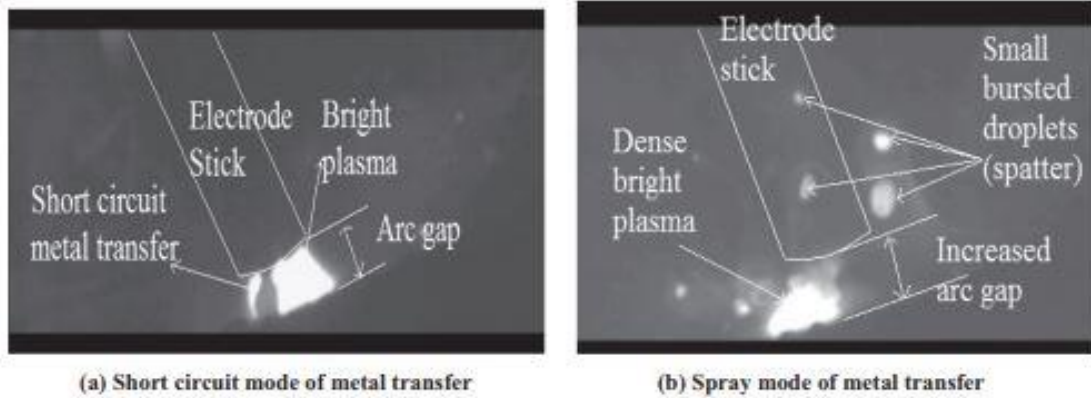


Figure 2-8: Different modes of metal transfer that take place in E6010 electrode [22]

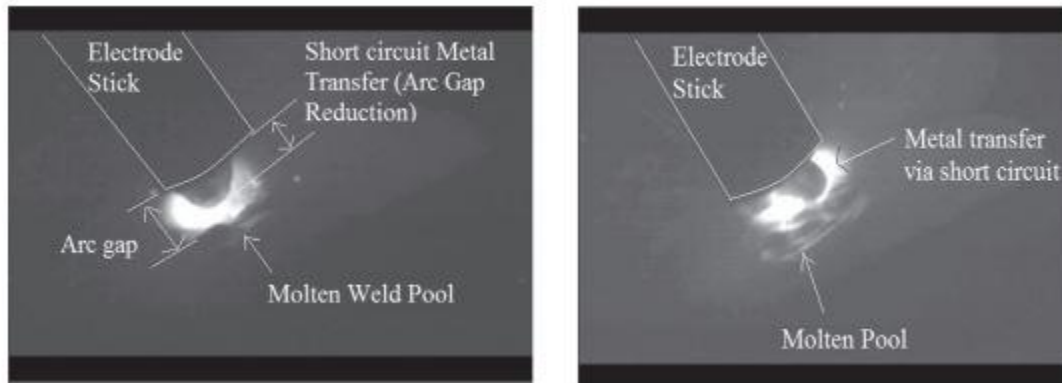


Figure 2-9: Short circuit metal transfer in E7018 electrode [22]

Previous research has discussed the mode of transfer in E6010, E7018. The industry guidelines published by the American Welding Society (AWS) in 1976 [23] concluded that it is difficult to establish the mechanism of metal transfer in SMAW, however, under optimal conditions the mechanism was observed to be a showery spray of metal and explosive droplets. Kumar et al. [24] used a digital storage oscilloscope (DSO) for data acquisition of voltage and current signals and a high-speed camera for observing the molten pool and metal transfer to investigate this issue. Based on the signals, Kumar et al. showed one can generate a Probability Density Distribution (PDD) in order to explain the metal transfer modes for the electrodes. The

voltage PDD obtained for E6010 and E7018 are given in the Fig 2-10 (a) and (b) respectively, which indicates three peaks for E6010, while two peaks are observed in the case of E7018. One of them represents the average voltage value and the other peak observed at a voltage value at which short circuit takes place, and this can be seen in Fig 2-9 where short circuit mode of metal transfer takes place. However, in the case of E6010, the additional peak occurs at a voltage higher than the set value, and they concluded that this peak was responsible for the explosive/spray transfer observed in the E6010 metal transfer shown in Fig 2-8 (b).

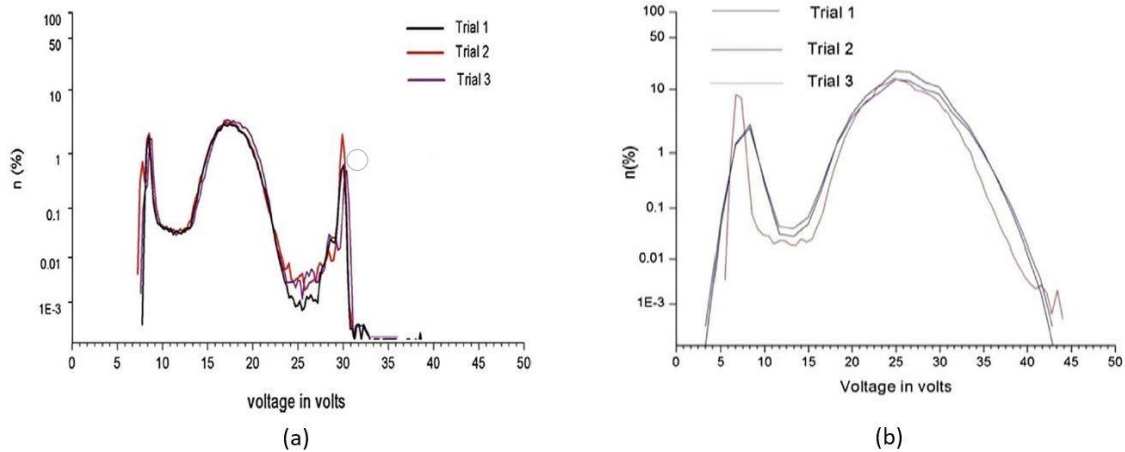


Figure 2-10: a) PDD of voltage signals of E6010; b) PDD of voltage signals of E7018 [24]

2.4 Welding Power Supplies

The welding power supplies that are under study are DC generator power supply and solid-state power supply. The similarity between the machines is that both of them run on diesel, which makes them the perfect choice of welding power supply for off-grid applications where high power electrical connections are not available. Both the power sources are suitable for a variety of welding processes including SMAW, TIG, FCAW etc., offering both constant current and constant

voltage outputs. Table 2-2 lists the technical specification of the machines for comparison, where both offer a similar range of performance. The two machines are different in the way they produce and control the current necessary for the welding process. The DC generator power supply provides a pure direct current through the rotation of electromagnetic windings on the motor shaft. Fig 2-11 illustrates the internal structure of the machine, which consists of a DC generator/dynamo. The generator consists of two working parts: rotor and stator; and one of them generates a magnetic field while the other has electrical windings. These windings are “tapped” into different combinations, which in turn controls the peak current during short circuit event [25]. The use of this mechanism to control the current results in a current waveform that has a triangular waveform, where the current reaches the peak gradually, as well as reduces to the set level gradually. This is shown in Fig 2-13 (a), which shows the graph of current (A) vs time (ms) for one of the short circuit events, during which there is a rise in the current value in order to restart the arc and continue welding.

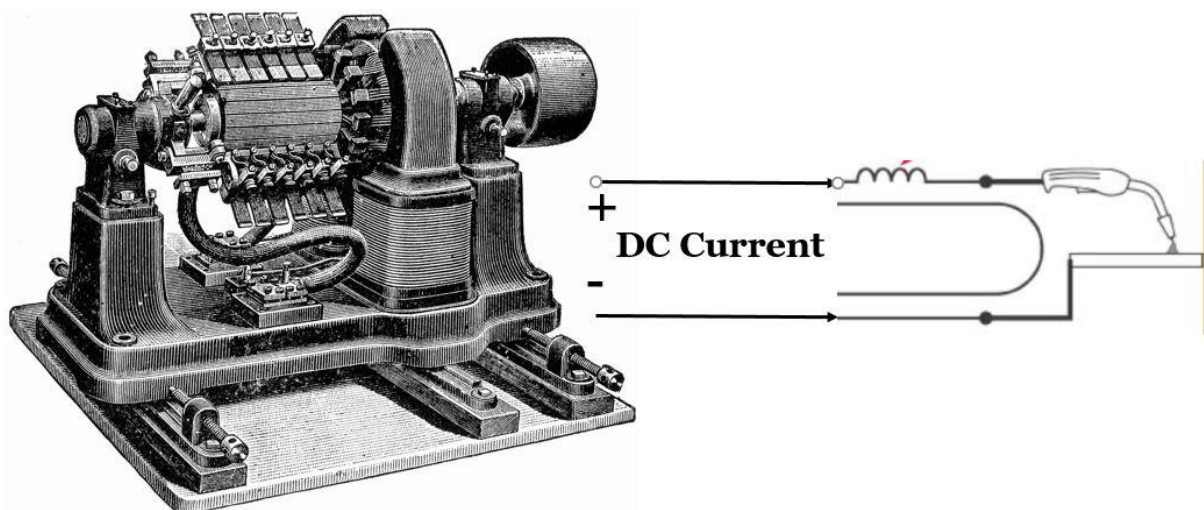


Figure 2-11: Internal structure of DC generator power supply [25]

The internal design of the solid-state power supply, are schematically shown in Fig 2-12. This power supply is different in the way it produces the current, where the power supply employs an alternator that produces Alternating Current (AC), which is then converted into direct current (DC) with the use of rectifier, which ‘chops’ the reverse flow of current through a rectifier, hence the term ‘chopper’ power supply used in industry. This direct current, is then precisely controlled by the use of Insulated-Gate Bipolar Transistor (IGBT) modules, which are responsible for combining high efficiency and frequencies of solid-state switches that regulates the amount of current that is supplied to the arc. This switch closure cycle has a frequency of at least 20kHz [26, 27, 28], which allows for the fast control of arc. This fast control of the current results in a nearly square waveform. Fig 2-14 (b) shows the graph of current (A) vs time (ms) for one short circuit event. This graph shows, how the use of IGBT modules result in highly accurate and fast control of the current, maintaining it at the set level with less variation, and with fast response to the short circuit by surging the current to a pre-set peak level and maintaining the current at this peak level for 4-5ms until the arc is re-established. This is different from what is observed in the waveform generated using the DC generator power supply. In case of the DC generator source waveform, the current starts rising as soon as the arc extinguishes, and gradually increases until the arc is re-established. This means that the peak current observed at each short circuit event need not be necessarily the same peak level.

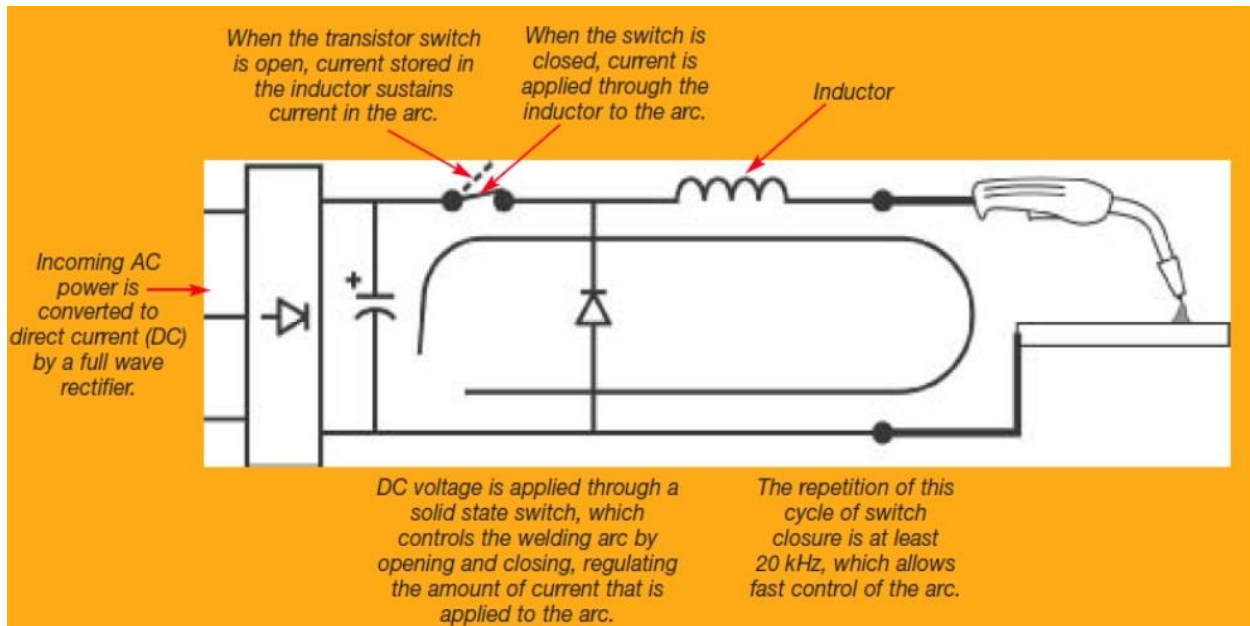


Figure 2-12: Internal components of solid-state power supply [28]

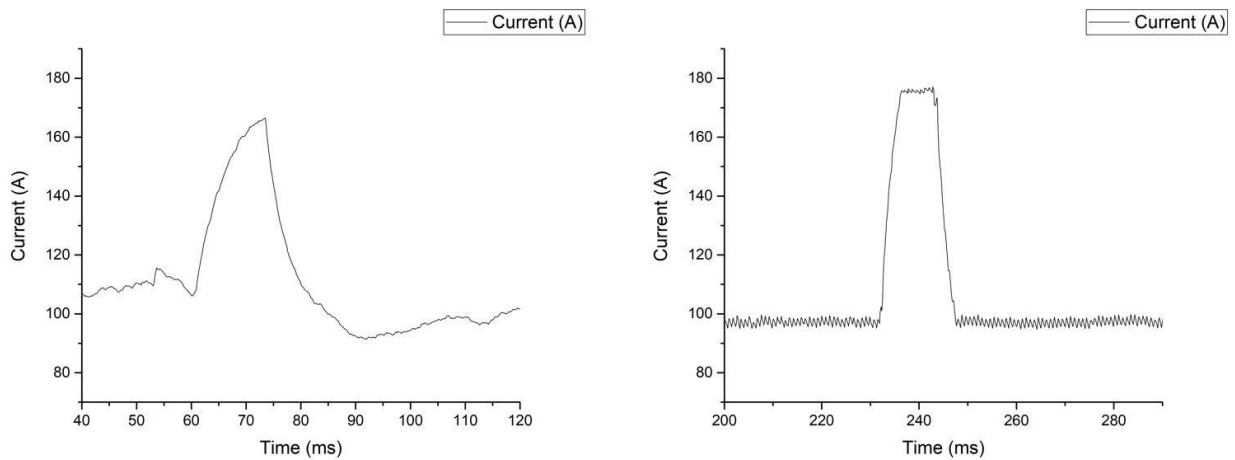


Figure 2-13: Current waveform during short circuit observed when using (a) DC generator; (b) Solid-state.

Research work in comparing a DC generator based power supply vs. a solid-state power supply for the shielded metal arc welding process have been performed by Vikram et al. [24]. They used an oscilloscope for data acquisition of voltage and current signals in the time domain to explain the different modes of metal transfer. Fig 2-15 (a) shows the oscillogram of current and

voltage when the welding was carried out using DC generator power supply, while Fig 2-15 (b) represents the current and voltage oscillogram when welded with the inverted based power supply.

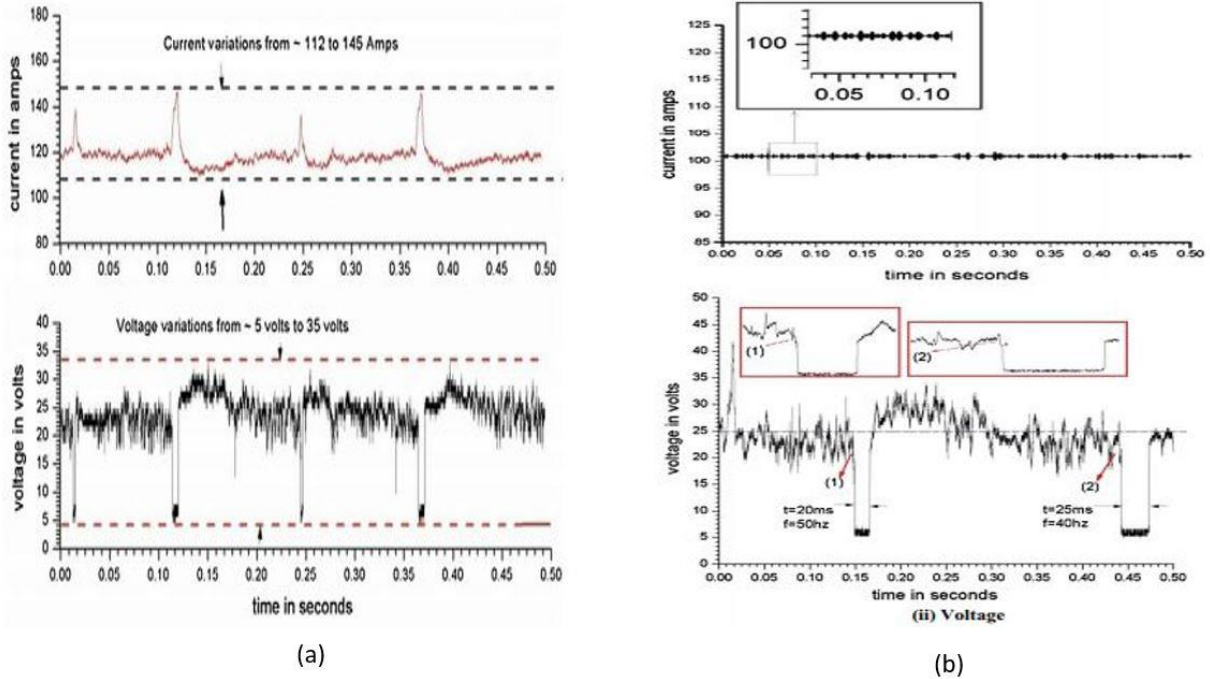


Figure 2-14: Current and Voltage Oscillograms when welded using (a) DC generator based power supply; (b) Inverter based power supply [24]

The primary difference that was noted was the difference in the current oscillograms where that a rise in current during short circuit events is observed with a DC generator based power supply, whereas there is no observable variation in the current level using the solid-state switching design, meaning the current value stays close to the pre-set value. This is because, in the solid-state based power supply, AC supply is rectified and fed into IGBT modules to produce a high frequency AC. This high frequency AC and fast response of IGBT modules suppresses the surge in the current level when there is a drop in the voltage. This paper concluded that current PDD could be used to compare the performance of the power supplies while the voltage PDD can be used to bring out the difference in the modes of metal transfer.

Chapter 3

Experimental Parameters

3.1 Welding Parameters

Table 3.1 lists the welding parameters that were used for the first set of experiments, where the weld type was bead-on plate and the experiments involved two different operators and two different electrodes-E6010 and E7018. These two electrodes are chosen for the reason that these come under the widely used category, where E6010 is used for root passes and E7018 is used for fill passes. The material used, for all the experiments in this study was 1020 plain carbon steel. In order to replicate the requirements in the field, where the welding is performed far away from the machine, 100 feet long welding cables were used for the study to reproduce the inherent inductance of cables that would be used. Unlike the digital control of current on the Solid-state power supply, the DC generator power supply cannot be set to a particular current level. Rather, this equipment has a coarse and fine current control knob. The coarse setting allows us to choose a range of current values; where 120-190A is the range used for all the experiments based on the recommendations for the electrode thickness used, which was 3.2 mm for all the electrodes. For more precise control, the fine current setting ranges from 0 to 100%; and this input parameter on the DC generator power supply were set at 20%, 50% and 80%. In order to achieve identical average current settings for the two power supplies, measurements were made at these three fine current settings with the DC generator power supply, and the output average current was recorded using a data acquisition system, and this value was set as the digital current setting for the Solid-state power supply. The average current value was again measured using the data acquisition system for the Solid-state

equipment, and verified to be the target setting on the controls. The welding was repeated three times at each current level to minimize the error.

Table 3-1: Welding Parameters for bead-on plate welding.

<i>Operator</i>	<i>Power Supply</i>	<i>Electrode</i>	<i>Current values (A)</i>
Inexperienced	DC generator	E6010	69
			84
			121
	Solid-state	E7018	82
			102
			138
Experienced	DC generator	E6010	75
			88
			124
	Solid-state	E7018	84
			107
			140

The next set of experiments involved replicating pipeline welding positions with the welding performed by an experienced pipeline welder. Table 3.2 lists the parameters for the welding of different positions as well as the gap bridge-ability test that was performed in the flat position. Gap bridge-ability test measures the length of weld that could be completed before the gaps become large for the operator to weld with ease. For the gap bridge-ability test, the 25 cm plates were kept close at one end with a tack weld, gradually increasing the gaps between the plates,

with a gap of 5 mm at the other end. Figure 3-1 shows the parameters and positions used to replicate pipeline welding. A typical welding procedure for pipeline applications will required multiple weld passes to fill groove, and often utilize the E6010 electrode for the first (or root) pass, while E7018 is used for the fill passes and E8010 for the final (cap) pass.

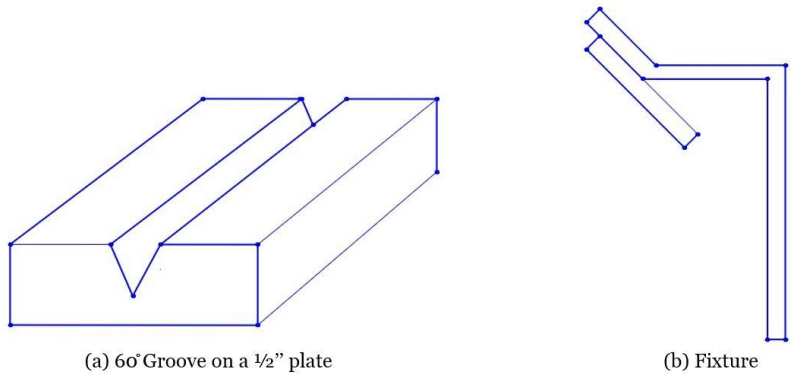


Figure 3-1: Fixture used to replicate pipeline welding.

Table 3-2: Welding parameters for experiments replicating pipeline welding.

<i>Operator</i>	<i>Power Supply</i>	<i>Welding Position</i>	<i>Electrode</i>
Experienced	DC generator	Downhill	E6010 E7018 E8010
		45 degree declined	E6010 E7018 E8010
		Flat (Gap Bridge-ability test)	E6010
	Solid-state	Downhill	E6010 E7018 E8010
		45 degree declined	E6010 E7018 E8010
		Flat (Gap Bridge-ability test)	E6010

Additional tests that were conducted included the calculation of melt-off rates, and welder hand position measurements using an accelerometer. Three operators with different experience

levels, namely Novice- non-certified welder with no experience, Intermediate- non-certified welder with at least one month experience, and Experienced- CoQ certified welder; performed the experiments for the calculation of melt-off rates with electrodes E6010 and E7018. The operator welded at constant welding speed for 45 seconds and the remaining electrode length was used to calculate the consumed electrode and thus, the actual melt-off rate of the electrode was extrapolated per hour. Five trials were performed at a particular current level to minimize the impact of error and random variations during welding. The accelerometer consisted of an apple smartphone, which was running “Accelerometer” app that collected the built-in accelerometer sensor data for the Z-axis at a rate of 20 Hz. A graph of acceleration vs welding time can be plotted and compared between the power supplies, for a particular current level to compare the amount of arc pressure generated at the electrode and reaction movements of the welder.

3.2 High-Speed Imaging

In this section, the imaging parameters are optimized to reveal the metal transfer phenomenon. In prior work, dos Santos [29] utilized a camera (FASTCAM Mini UX50, Photron, USA), with a frame rate of 5000 fps (frames per second) and exposure settings of 3.91 and 20 μ s, and it was noted that the primary emission of the ionized iron vapor, and arc plasma could be distinguished using optical narrow band pass filters of 515nm and 900 nm respectively. This is shown for comparison in Fig. 3-2 and 3-3.

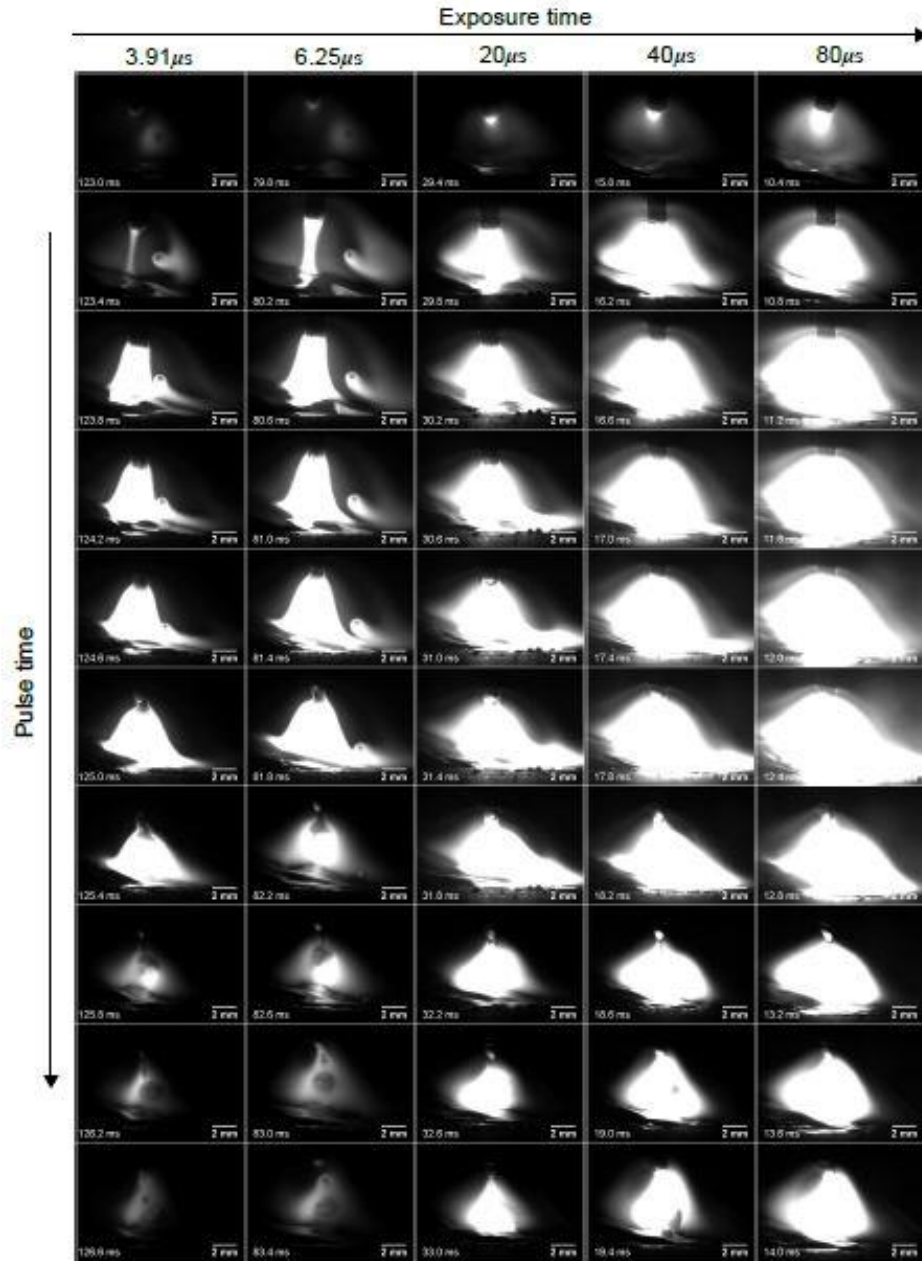


Figure 3-2: Arc appearance for aperture $f/22$ using 515 nm wavelength band pass filter for different exposure times [29].

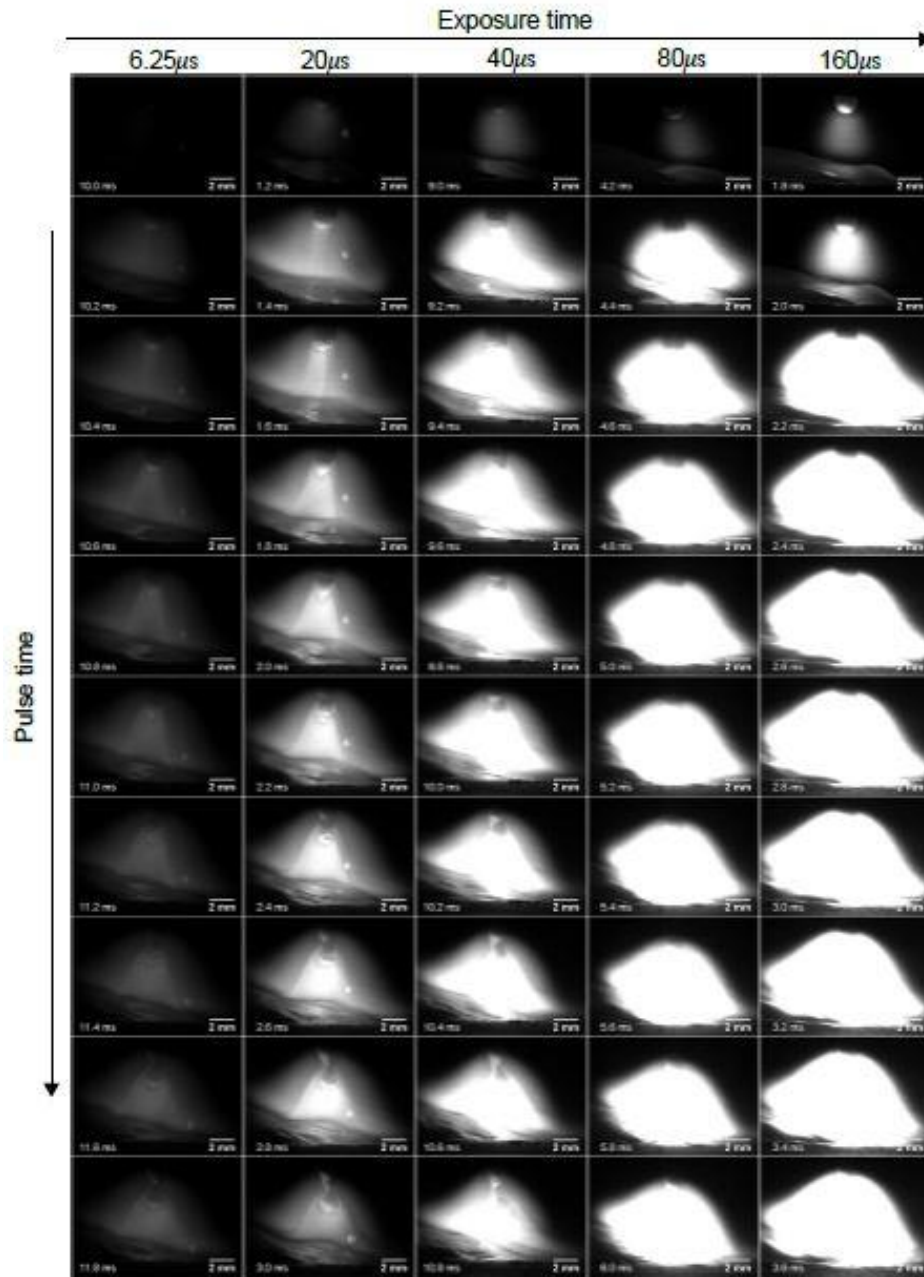


Figure 3-3: Arc appearance for aperture $f/22$ using 900 nm wavelength band pass filter for different exposure times [29].

Chapter 4

Results and Discussions

4.1 Voltage and Current Oscillograms and Histograms

The first set of experiments involved bead-on plate welding performed with two electrodes: E6010 and E7018, and with two operators: an *inexperienced* (uncertified welder with less than 1 month experience), and an *experienced* (CoQ) welder qualified per the Canadian Standards Association. Current and voltage signals were recorded using the NI DAQ system over a period of 2 seconds with a data collection frequency of 10 kHz. The oscillograms that were generated are shown in Fig 4-1. For most of the tests, it was important to gather data for at least two welders since SMAW is a completely manual process controlled by the user. Also, the comparison between a rather novice and expert provided a deeper perspective into whether there are any drastic differences in performance arising from the experience base. Thus, potential differences in equipment response will only be detected if they persist even with potentially incorrect technique applied by the novice, versus the possible strong habits of the expert user. The intention here was to reveal the differences in performance, which are most likely attributed to the power supply design rather than welder technique.

The plot in Fig 4-1a show the current and voltage oscillograms when the DC generator power supply was used, while the plot in Fig 4-1b show the oscillograms generated using the solid-state power supply. The inexperienced operator performed the welding using a E7018 electrode, and the current setting was 102 A for the solid-state power supply, which matched the average current produced using the DC generator power supply when the current range 120-190 A with a

50% fine current setting was selected. The key differences to be noted from the two plots are the frequency of short circuit events that happen over the 2-second period, and the variation of current during welding (background) as observed in the current oscillogram. A short circuit event occurs when the metal droplet at the tip of the electrode makes contact with the plate, which makes the voltage approximately zero. When this happens the power supply reacts by surging the current to particular value to reinitiate the arc and break the contact and thus, depositing the metal. When welding was carried out using the Solid-state power supply, more short circuit events were observed in comparison to the DC generator power supply, as shown by the oscillograms, which is also supported by high-speed video recordings. Likewise, the frequency of the short circuit events, when using the E6010 electrode with the Solid-state power supply were significantly more often than observed with the DC generator, as can be seen from the current and voltage oscillograms shown in the Fig 4-2. The current level was set at 69A and with an inexperienced operator performing the welding.

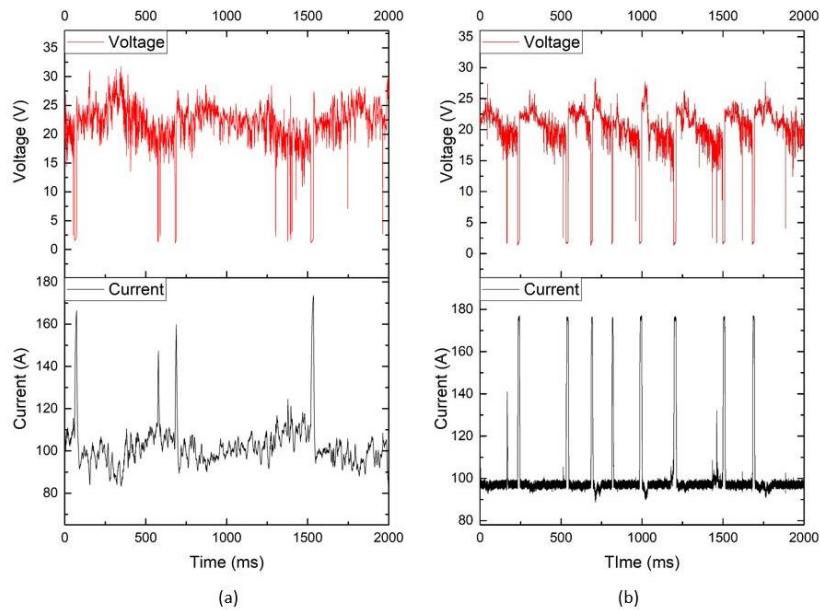


Figure 4-1: Voltage and Current Oscillograms generated during welding with E7018 electrode by an inexperienced operator, using (a) DC generator (b) Solid-state power supply

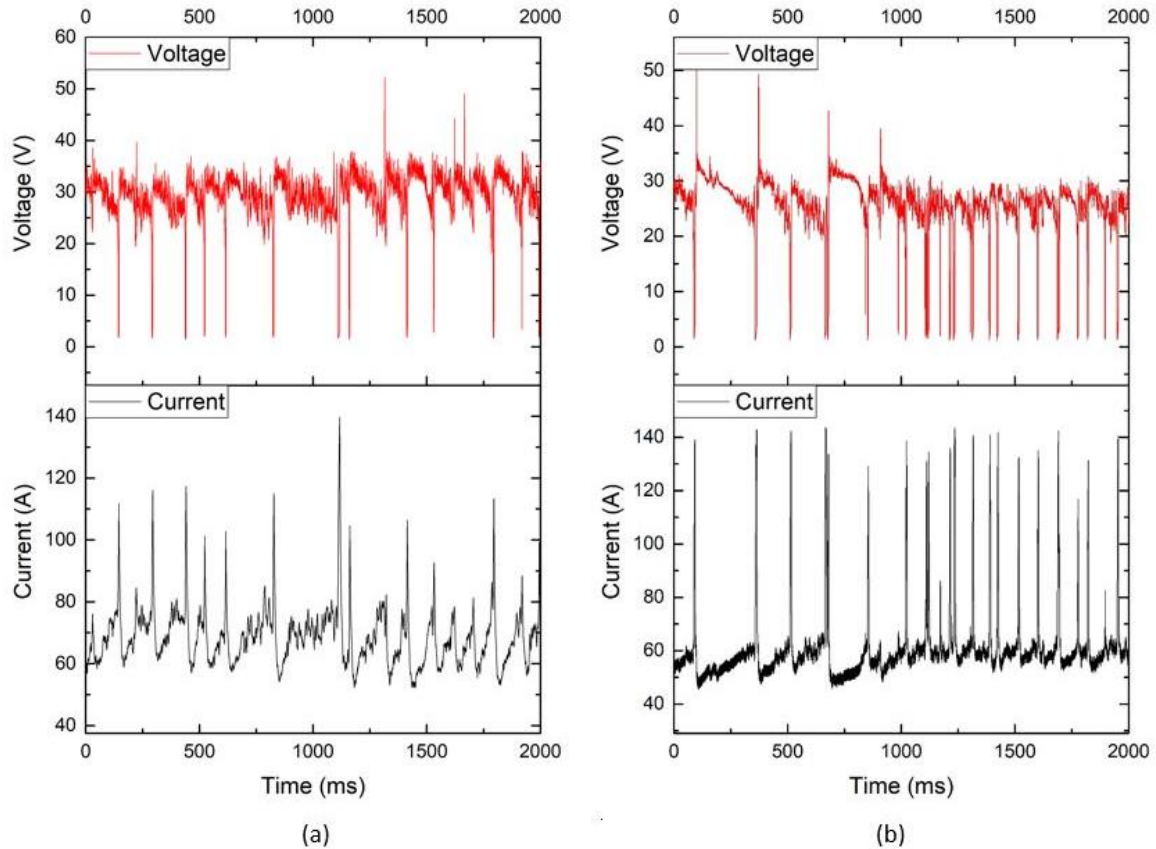


Figure 4-2: Voltage and Current Oscillograms generated during welding of E6010 by an inexperienced operator.
using (a) DC generator (b) Solid-state power supply

From Fig 4-1 and 4-2, comparing the current oscillograms between the power supplies, a difference could be observed during the short circuit pulses. When there is a dip in voltage, the power supply responds to it by surging the current to a peak level to re-initiate the arc. With the DC generator power supply, the peak current observed at every short circuit has a slightly different profile, unlike the Solid-state power supply where the current surged to a nearly ideal constant value for every short circuit. The reason for this difference is the current waveform the power supply generates during short circuit, as can be seen in Fig 4-3. Since DC generator power supply produces a smooth and gradual increase in the current until the arc is re-initiated, the peak current value depends on the duration of the short circuit. The longer the duration of short circuit, the higher the value of current. However, in the Solid-state power supply, more advanced circuitry

using the IGBT modules, results in a response which can quickly ramp up to the peak current during a short circuit. This produces a very steep increase in the current, and the current reaches the constant (machine’s pre-set value) peak level within 4 to 5 millisecond. This means that regardless of the duration of the short circuit, the peak current level is not affected during different short circuit events.

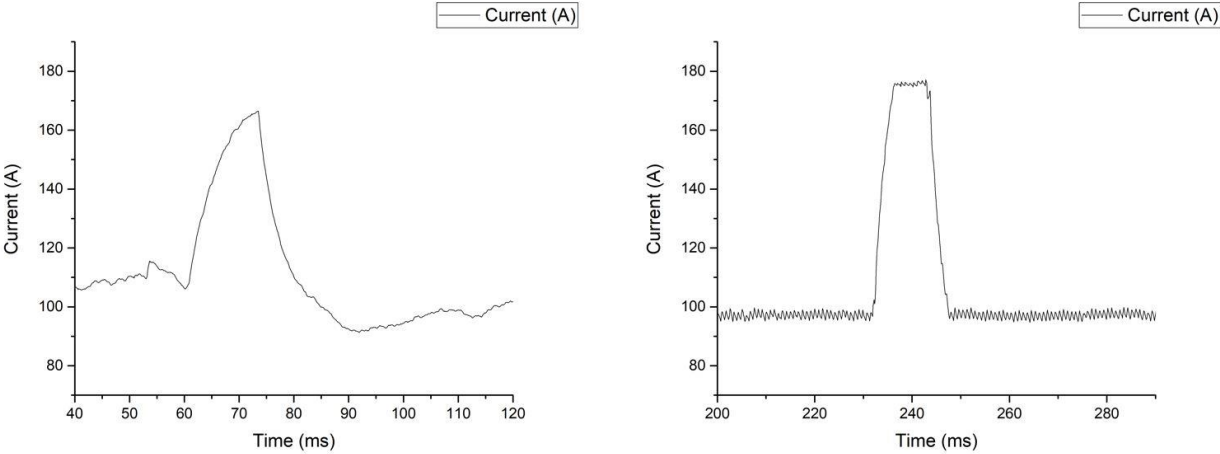


Figure 4-3: Current waveform during short circuit with (a) DC generator, (b) Solid-state power supply.

Fig 4-4 shows the instantaneous rate of change of current for both the power supplies. From, Fig 4-3 and 4-4, the fast response to current during short circuit can be noted for the Solid-state equipment. Comparing the derivative of the current for both the power supplies, two differences can be observed; firstly, the range of the current derivative, secondly, the central band. Since Solid-state uses IGBT modules to control current, we can expect a large current derivative value during short circuit.

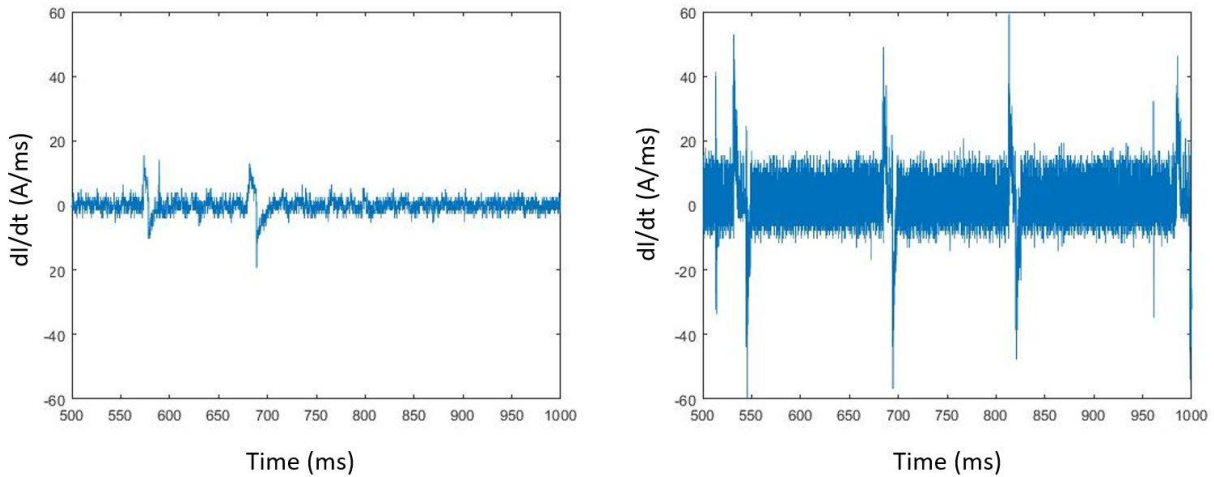


Figure 4-4: Current derivative plots when welding was performed with (a) DC generator, (b) Solid-state.

The second difference is observed in the stability of the central band. For example, with the DC generator power supply, more gaps can be observed in the central band of the current derivative. This is because of the fact that the variation of current around the average value is large as compared to the variation observed in the current value for the Solid-state power supply. The fast switch closure with a frequency of at least 20 kHz [26, 27] controls the current every millisecond and therefore, variation in current during the background circuit time is minimal. Vikram et al. [24] mentions that a good power supply will try to reduce the variation in current level, since a constant current setting is normally intended for SMAW. The wider variation in the current value can also be noted from the histograms generated from the current signals for both power supplies as shown in Fig 4-6. Even though the solid-state power supply does offer a better constant current output than DC generator power supply, a rapid increase in current makes the arc less stable. The fast increase in current is related to a low value of inductance [30] and this can be seen from Figure 4-6, which shows the effect of inductance on the increase in current during a short circuit transfer. Due to the rapid increase in current when there is a dip in voltage, the arc is more unstable and excessive spatter occurs. However, adding inductance to the circuit increases

the current in a controlled and gradual manner, which makes the arc more stable, reducing the amount of spatter.

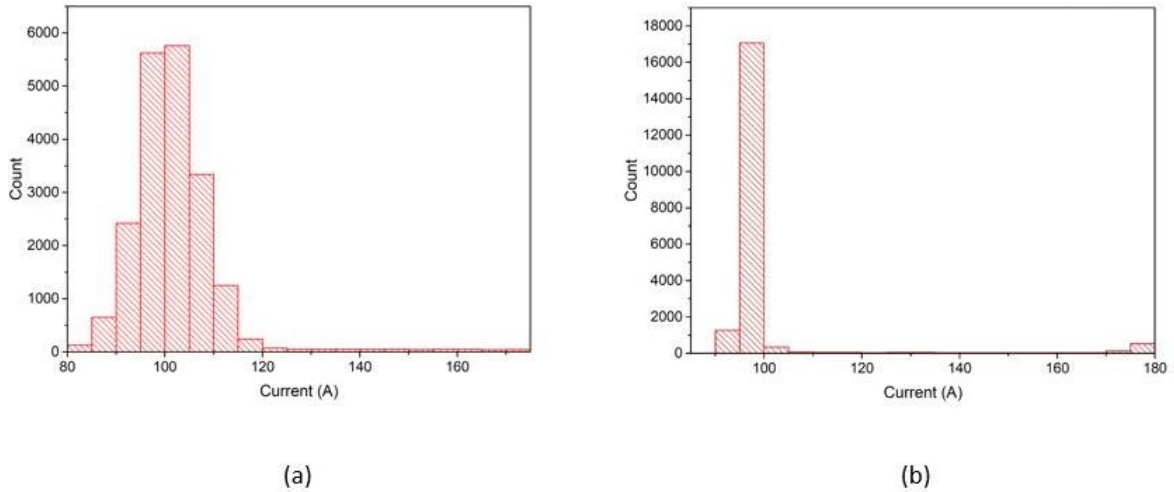


Figure 4-5: Histograms generated with current signals when welding was performed with (a) DC generator, (b) Solid-state by an inexperienced operator.

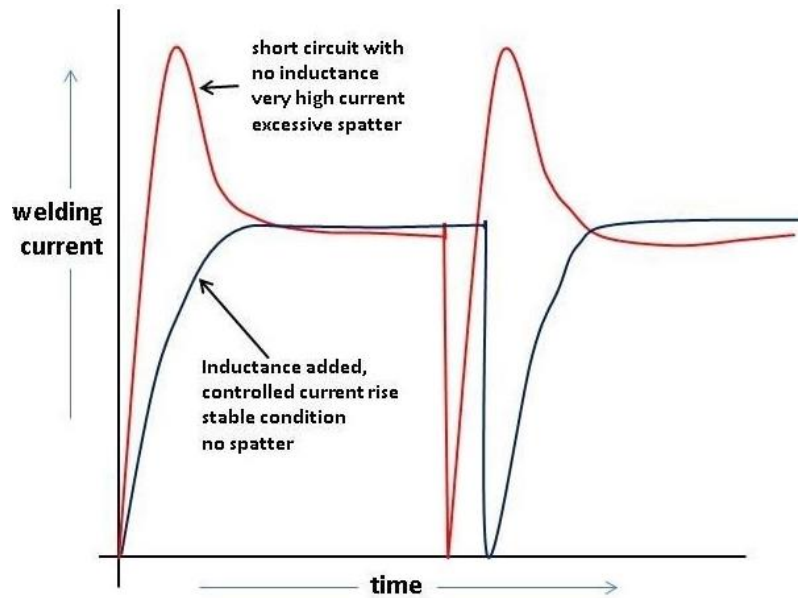


Figure 4-6: Effect of Inductance on current during short circuit event [30].

Since SMAW is a manual process, the current and voltage signals are not only affected by the power supply, but also the welder inputs. Therefore, an experienced welder repeated the experiments performed by the inexperienced operator, and the current and voltage oscillograms

are compared to reveal this influence, so that any differences observed between the power supplies can be confirmed to be a characteristic of their design. Figure 4-7 shows the current and voltage oscillograms when an experienced operator performed welding with an E7018 electrode, while Figure 4-8 shows the current and voltage oscillograms when E6010 was used. Comparing the oscillograms generated by an inexperienced operator vs an experienced operator it can be clearly seen that the difference observed in the short circuit frequency between the two machines, is not affected by the characteristic of the machine, rather is affected by operators technique. Analyzing Fig 4-1, 4-2, 4-7 and 4-8, the shapes in the waveforms are similar for the two designs, and we can find that the oscillograms are mainly affected by the characteristics of the power supply remain regardless of the operator.

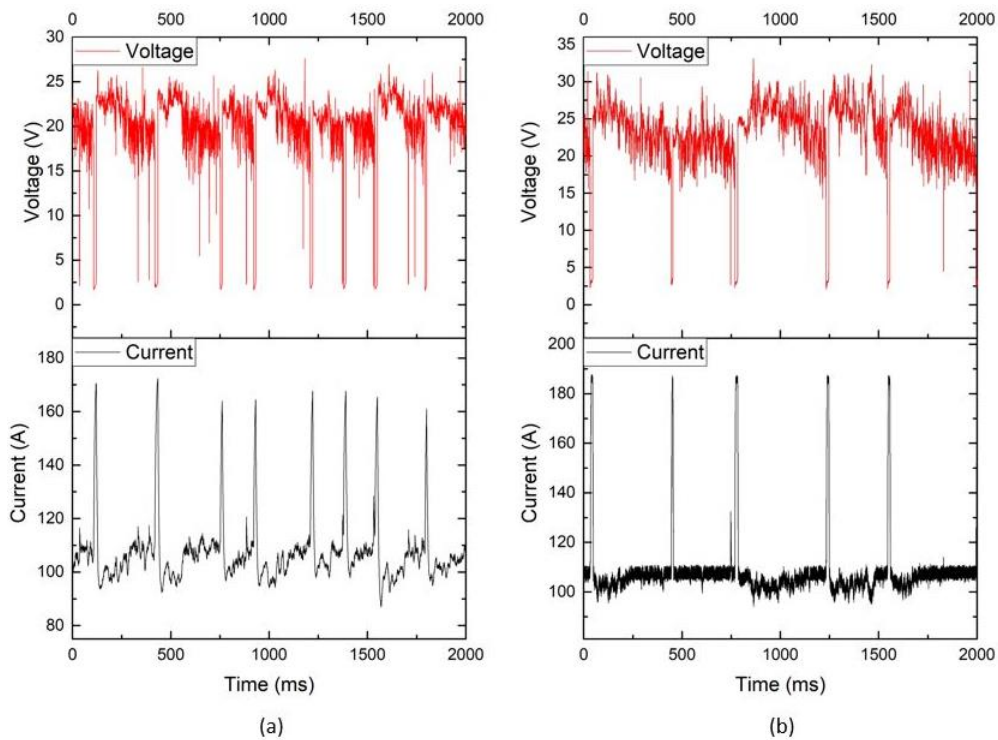


Figure 4-7: Voltage and Current Oscillograms generated during welding of E7018 using (a) DC generator: (b) Solid-state by an experienced operator

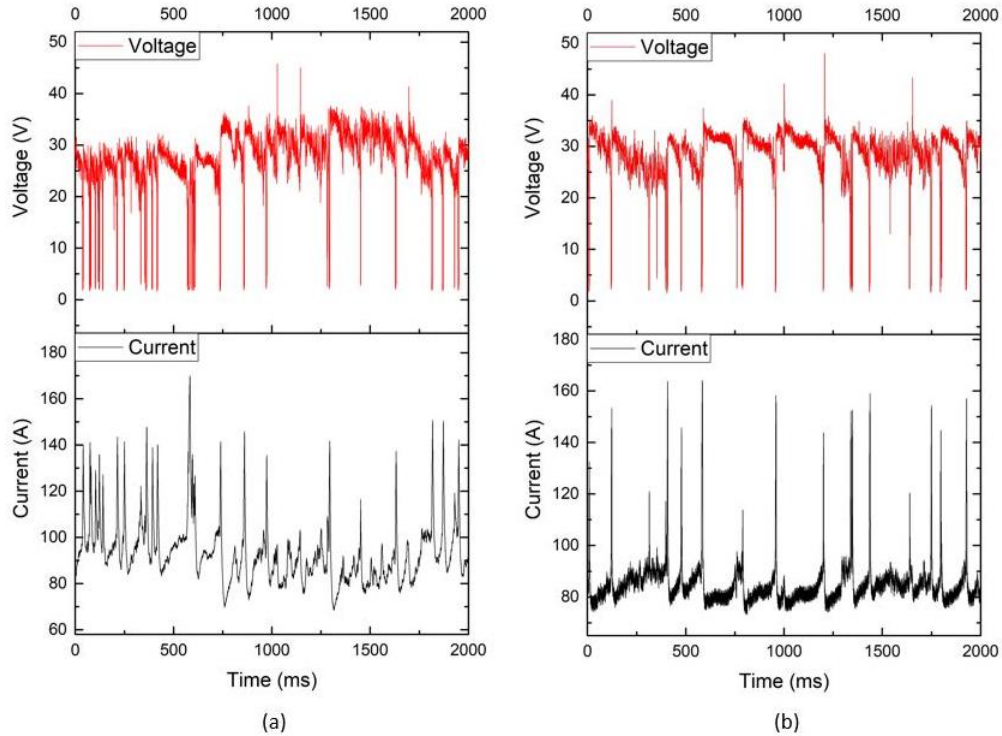


Figure 4-8: Voltage and Current Oscillograms generated during welding of E6010 using (a) DC generator; (b) Solid-state power supply by an experienced operator.

4.2 Heatscatter (Voltage/Ampere) Plots

This section deals with voltage/ampere plots that specify the normal operating current and voltage range, which in turn, gives important details about the characteristics of the power supply. The current and voltage signals collected over a period of 2 seconds with 10 kHz frequency provides a total of 20,000 data points that are used to generate a heatscatter plot with an intensity scale that describes the frequency of the points in an area. These V/I plots will be referred to as heatscatter plots and are generated by a Matlab code given in Appendix A. The intensity bar given on the plot indicates the amount of points present in the vicinity of a colored point. Figures 4-9 and 4-10 show the heatscatter plots generated with voltage and current signals, when bead-on plate welding was performed with E7018 by an inexperienced and experienced operator respectively.

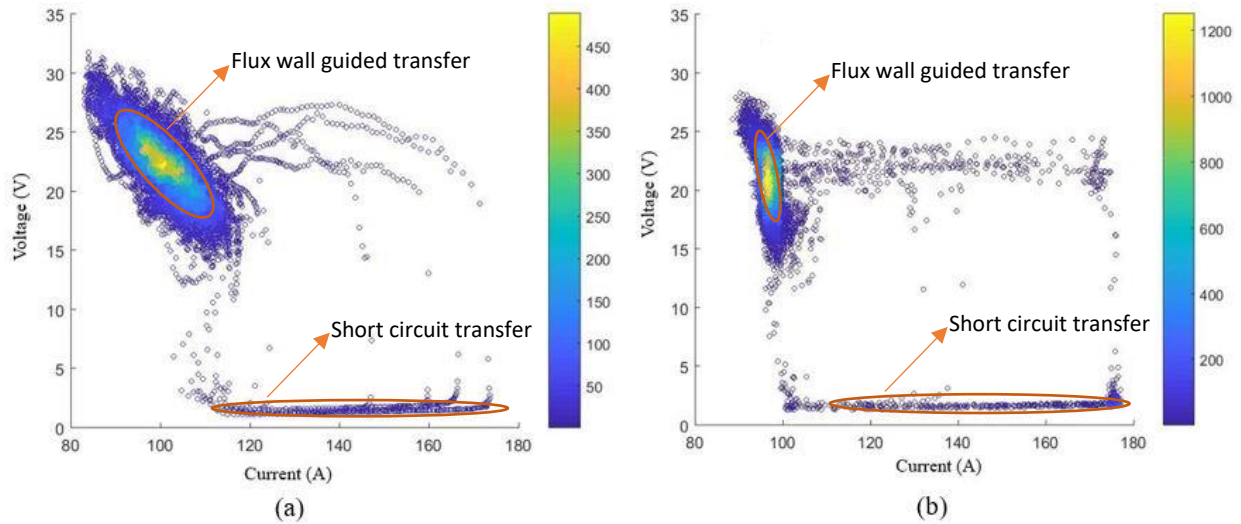


Figure 4-9: Heatscatter plots generated from current and voltage signals, when welding was performed with E7018 by an inexperienced operator using (a) DC generator, (b) Solid-state power supply

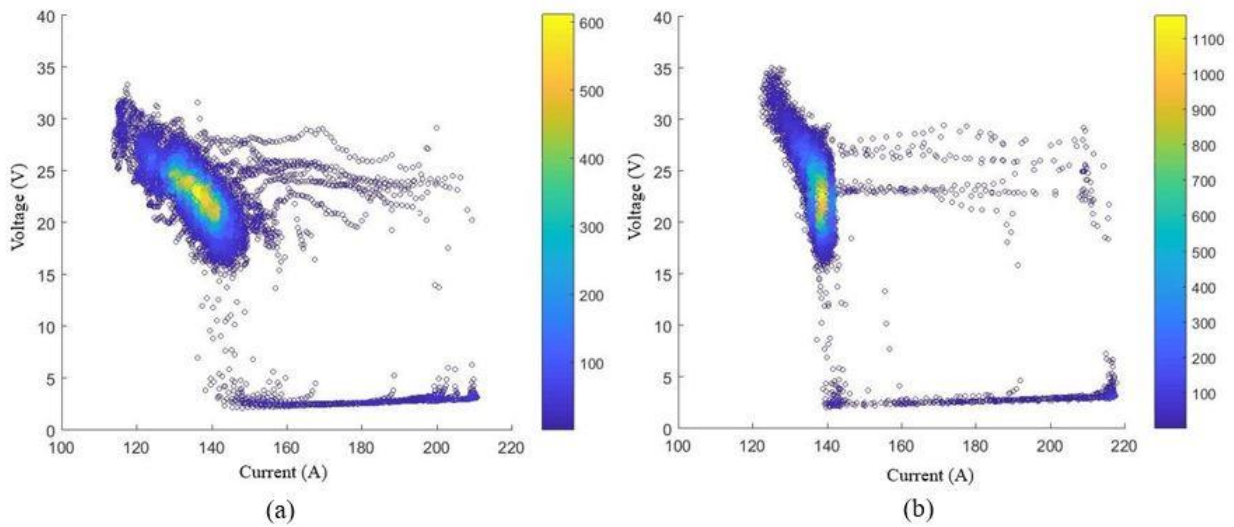


Figure 4-10: Heatscatter plots generated from current and voltage signals, when welding was performed with E7018 by an experienced operator using (a) DC generator, (b) Solid-state power supply

The difference between the two power supplies are plotted as the central region of the high intensity points, which shows the operating voltage and current range. Operating range, is defined here as the current and voltage values supplied by the power supply during the stable arc period of the welding corresponding to the range where 65% of points are concentrated. The other low

intensity points can be considered as outliers in order to differentiate between the characteristics of the power supply and how they affect the V/I plots. It should also be noted that, the spread of points in the central region deviates around either side of the average current value in case of the DC generator power supply. However, using the Solid-state power supply provides a central region with a distribution of points on only one side of the pre-set current level (average current) with a sharp cut-off at the average current level. The other difference observed in Fig 4-9 and 4-10, is the range of current values observed when the voltage is close to zero (the short circuit period). When the DC generator power supply is used, we observe from the plot that current can take any value between the average current and peak current, when there is a dip in voltage. However, the Solid-state equipment exhibits an accumulation of points at a particular current level during short circuit period. However, analyzing the oscillograms from the previous section, it was found out that the frequency of short circuit is not a characteristic of the power supply, and was affected by the operator influence. Therefore, the key difference demonstrated by the heatscatter plots is the central distribution of points.

The heatscatter plots shown above are generated from current and voltage signals recorded for bead-on plate welding. However, the application for which these power supplies are used will heavily involve pipeline welding and field structural welding. As the operator influence was responsible for change in short circuit frequency and not the power source, the orientation or electrode position in which welding is performed could affect these plots, and the trend observed thus far, may be affected by this factor. As mentioned in Chapter 3, pipeline welding was replicated, with the set ups shown in Figure 3-1, by an experienced pipeline welder, where the joints were made at a 45° angle in the downhill direction. The welding was performed with three

electrodes, E6010 for the root pass, E7018 for the fill passes and E8010 for the cap pass and their heatscatter plots are given in Figures 4-11, 4-12 and 4-13 respectively.

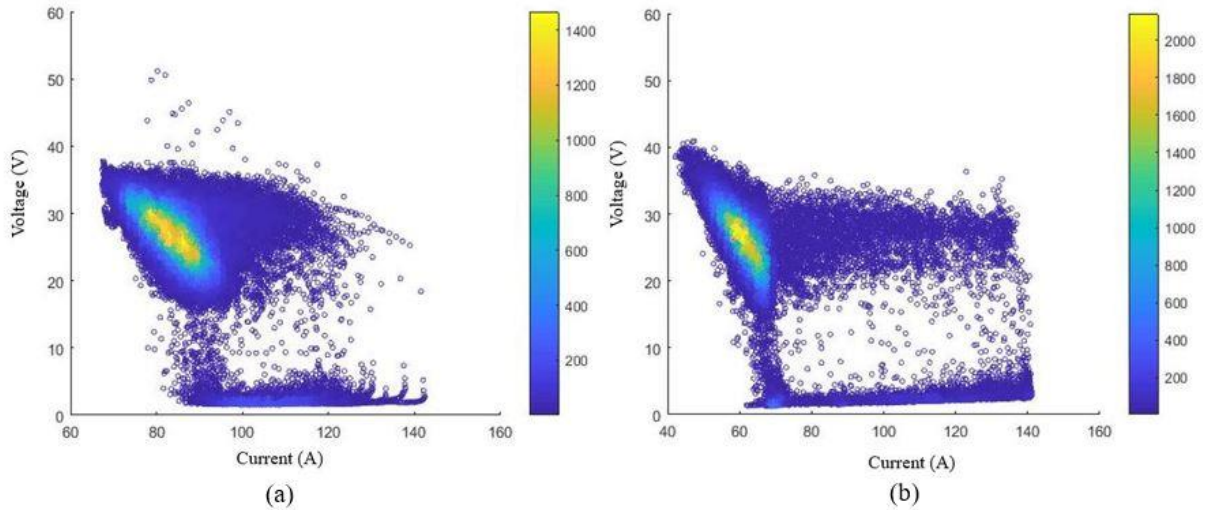


Figure 4-11: Heatscatter plots for welding performed at 45° downhill with E6010 using (a) DC generator, (b) Solid-state power supply

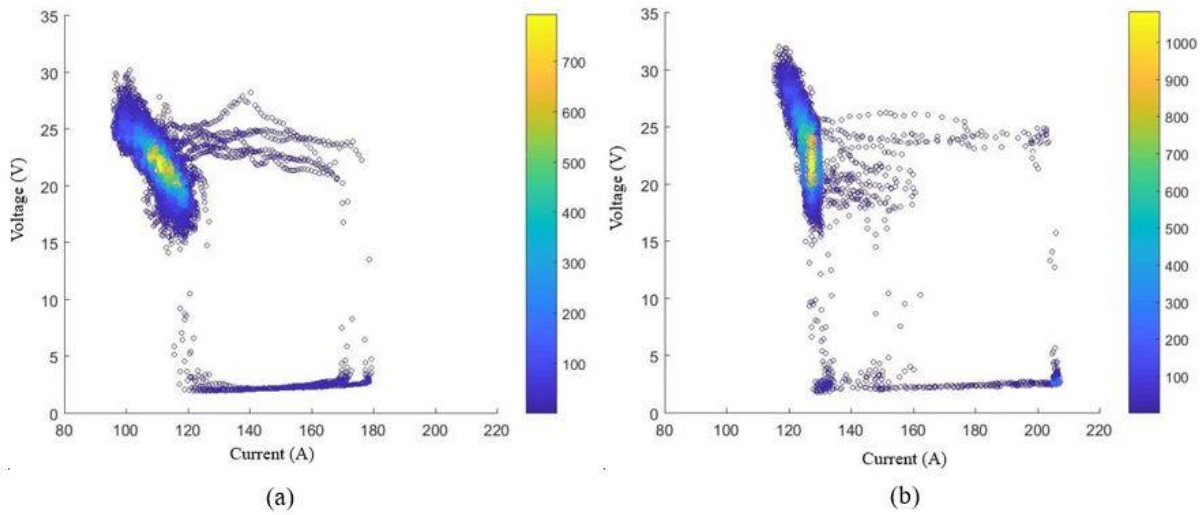


Figure 4-12: Heatscatter plots for welding performed at 45° downhill position with E7018 using (a) DC generator, (b) Solid-state power supply

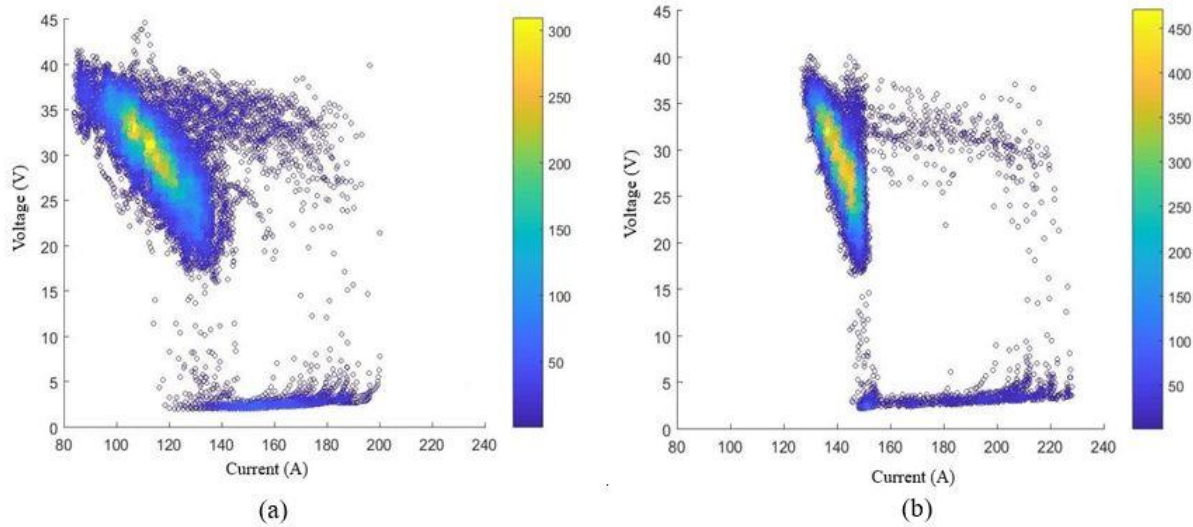


Figure 4-13: Heatscatter plots for welding performed at downhill position with E8010 using (a) DC generator, (b) Solid-state power supply.

Analyzing the heatscatter plots involving different electrodes, positions, operators and machines, we can differentiate the characteristics of the power supply regardless of the experience of operator, choice of electrode or position. The common difference observed across all the heatscatter plots discussed thus far, relates to the spread of central region and the maximum intensity value mentioned in the intensity bar. It can be seen that the value of the intensity bar using the Solid-state equipment is greater than that of the DC generator, which is associated with a narrow current operating range. The region of concentrated points is approximated to an ellipse containing 65% of the scattered data points, which will give the amount of current and voltage range, as shown in Figure 4-14 below. This ellipse would contain the current and voltage values supplied for most part of the welding and it is a characteristic of the power supply. The current operating range is 35 A for the DC generator power supply, while it is only 21 A for the Solid-state, and the voltage range is observed to be higher in case of Solid-state power supply. Since, voltage is affected by the arc length and with support of high dynamic range videos; it is safe to

conclude that DC generator power supply provides a tighter arc as commented by the welders who preferred DC generator power supply. Since the Solid-state power supply attempts to maintain a constant current level, it does so by reducing the flexibility for operator as the machine tries to control the arc, thereby making it potentially more difficult for welders to work with continuously for long periods. The higher arc force (uneven pressure at the tip of the electrode), observed in the high-speed videos, could be also related to the steep fall in current value after the arc is re-established which, explains the longer voltage range observed with the Solid-state power supply. The current operating range with DC generator power supply being greater than that of Solid-state explains the higher melt-off rate for the same average current, which will be discussed in Section 4.4.

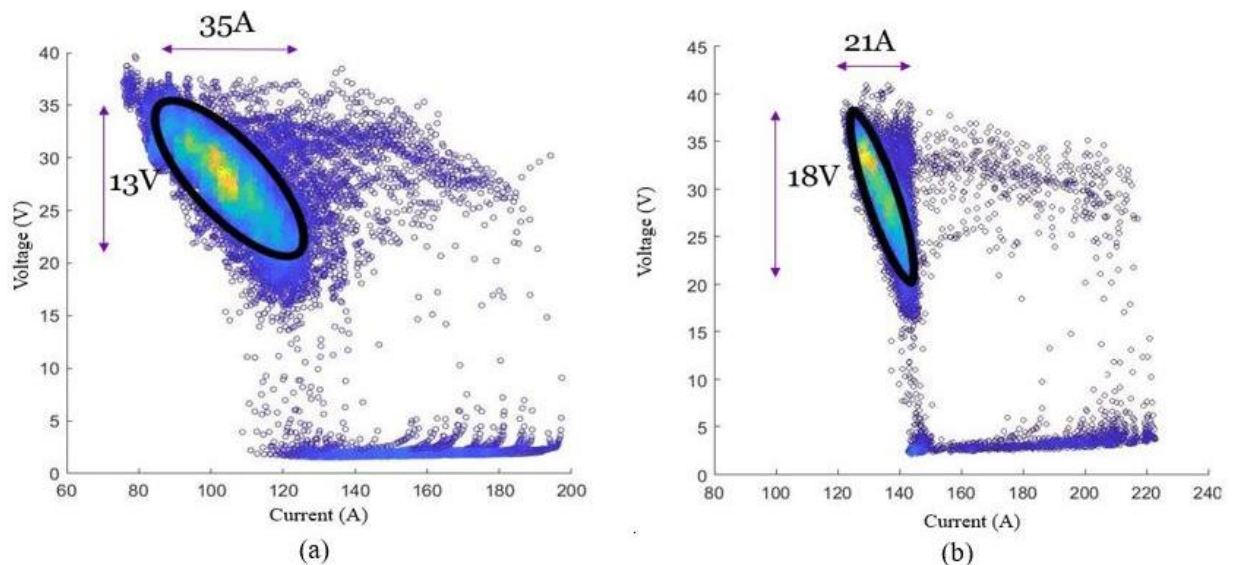


Figure 4-14: Region of concentrated points approximated to ellipse when welded using (a) DC generator, (b) Solid-state

4.3 High Speed Imaging

This section deals with high speed imaging which can be used along with the voltage and current oscillograms to explain the metal transfer modes present in shielded metal arc welding.

Figure 4-15 shows series of high-speed images synchronized with current and voltage signals to show a short circuit transfer. The high speed images of a short circuit event happening with either of the machines, can be compared to explain if there is a difference in the metal transfer, since it is known that the current oscillograms are different for the two power supplies. During the short circuit, the arc is extinguished followed by the formation of a droplet and detachment of this droplet. Figure 4-16 shows a series of high speed images during a short circuit event when E6010 was used. The type of transfer that happens in this case is explosive transfer and the higher voltage range observed in the voltage oscillograms in Figures 4-2 and 4-8 regardless of the power supply, is responsible for this explosive transfer.

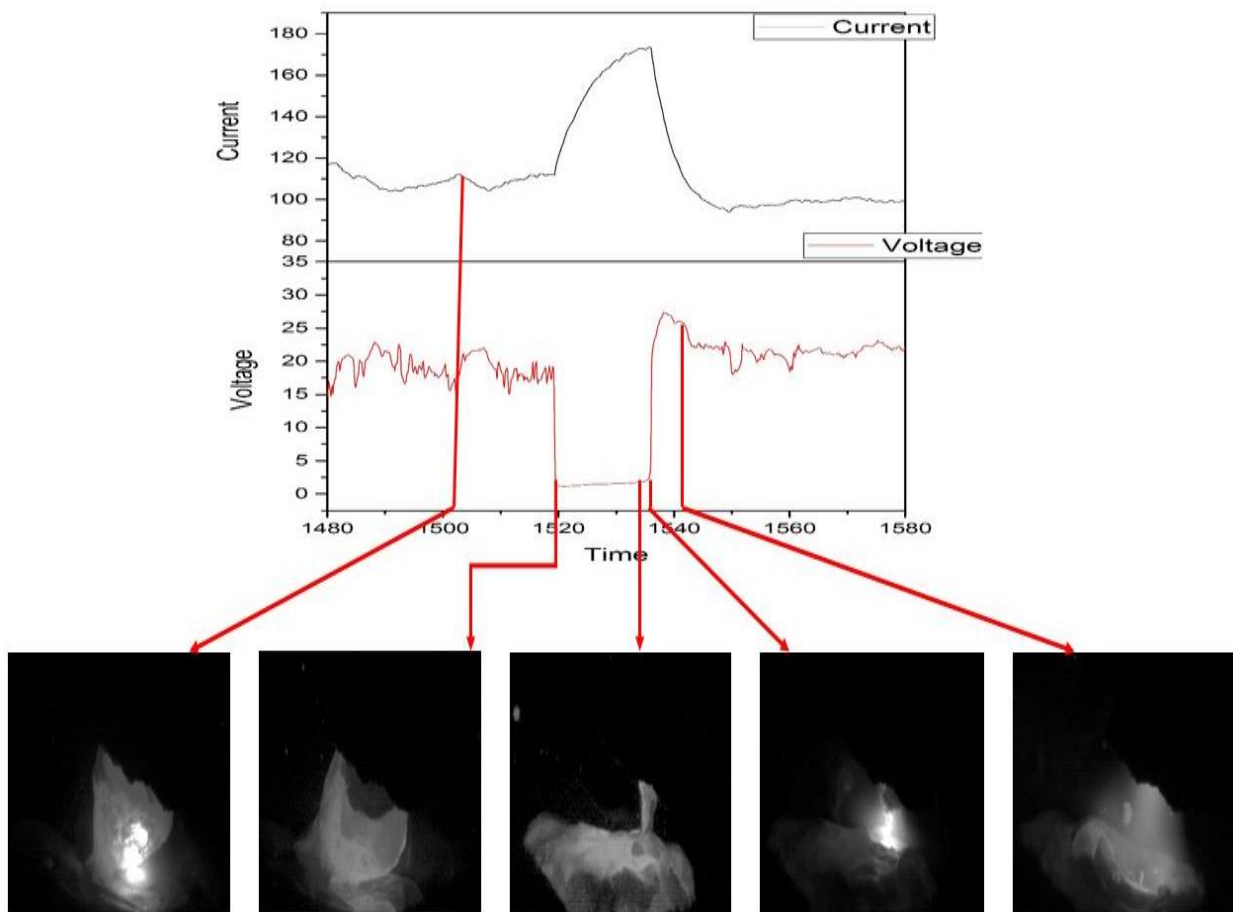


Figure 4-15: High-speed images synchronized with current and voltage signals to explain a short circuit transfer.

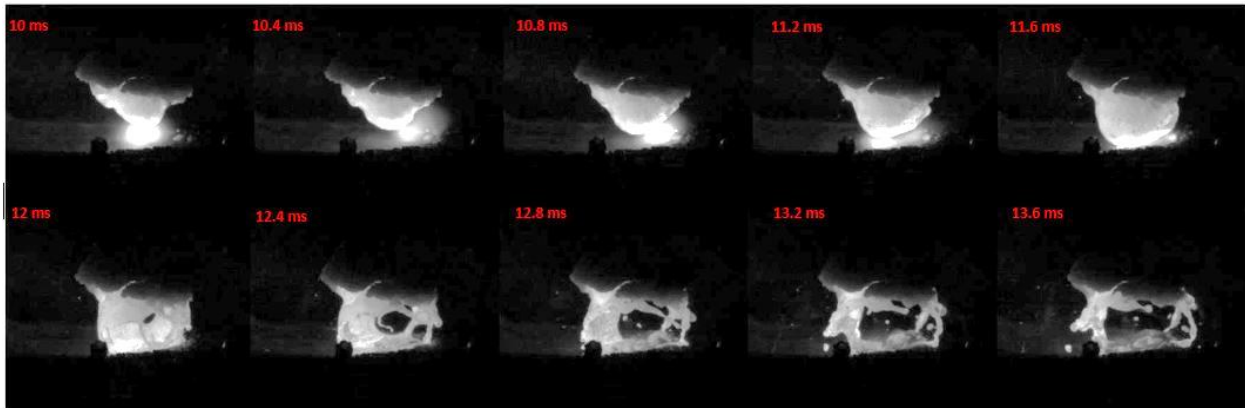


Figure 4-16: Series of high speed images during a short circuit event; Solid-state power supply, E6010 and Inexperienced operator.

When the welding was performed using E7018, the high speed video showed that, unlike E6010 where short circuit and explosive transfer are the primary means of metal transfer, flux-wall guided transfer seemed to be the predominant mode for the E7018 electrode with occasional short circuit transfers. This explains why the short circuit frequency observed with E7018 is less than that of E6010 regardless of the operator or power supply. Figure 4-17 shows the series of high speed images recorded during the flux-wall guided metal transfer of E7018.

It is important to explain and differentiate these modes of metal transfer between the two electrodes because of the following reason. As explained earlier, E6010 exhibits short circuit and explosive transfers, neither of which is affected by the characteristics of power supply. However, in the case of E7018, since flux-wall guided transfer is the predominant mode, there is a difference in the way detachment takes places depending on the power supply. Even though a high-speed camera with a 900nm filtered lens does clearly show the metal transfer, it is difficult to distinguish these modes between the power supplies and therefore, a 515nm filtered lens was used to observe

the difference. Fig 4-18 shows the series of high speed images recorded using a 515nm lens for the welding performed with the DC generator power supply while Fig 4-19 represents that of the Solid-state power supply.

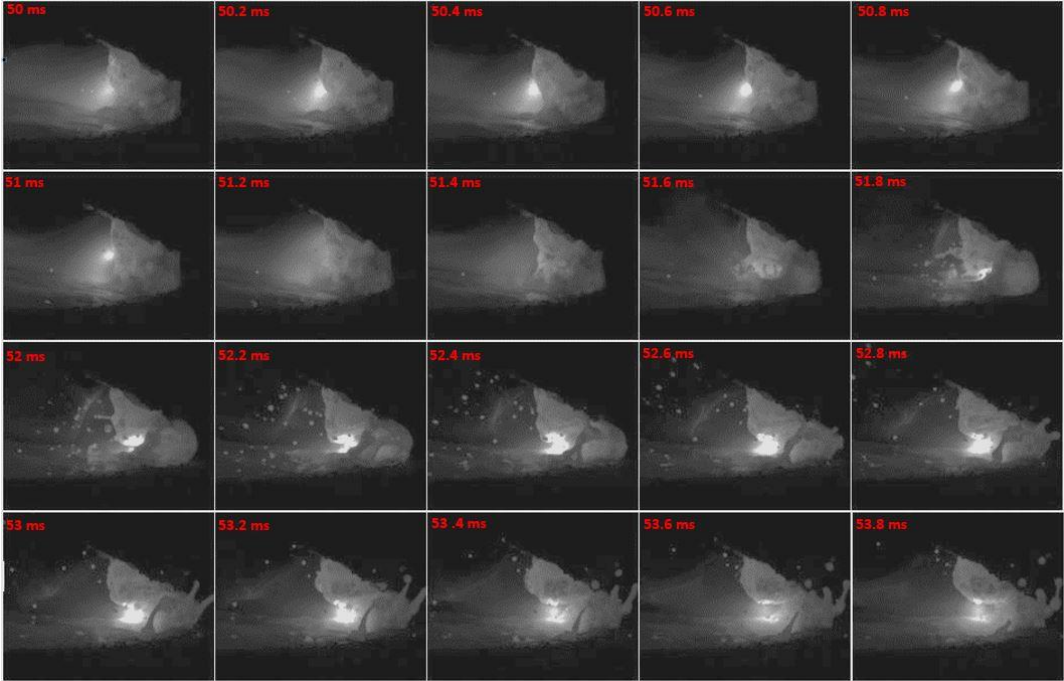


Figure 4-17: Series of high speed images to explain the flux-wall guided metal transfer; Solid-state power supply, E7018 and inexperienced operator.

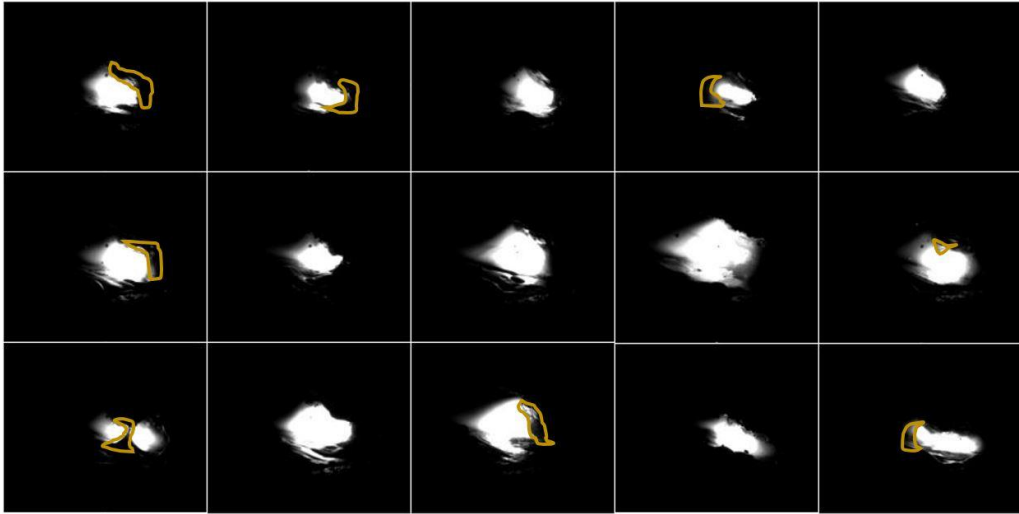


Figure 4-18: High-speed images recorded with 515nm lens for E7018 using DC generator power supply.

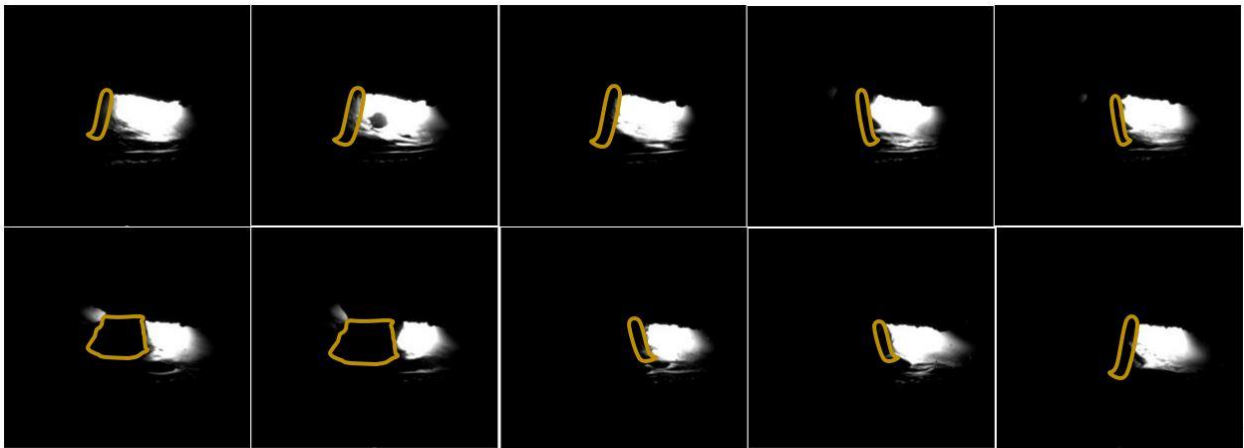


Figure 4-19: High-speed images recorded with 515nm lens for E7018 using Solid-state power supply.

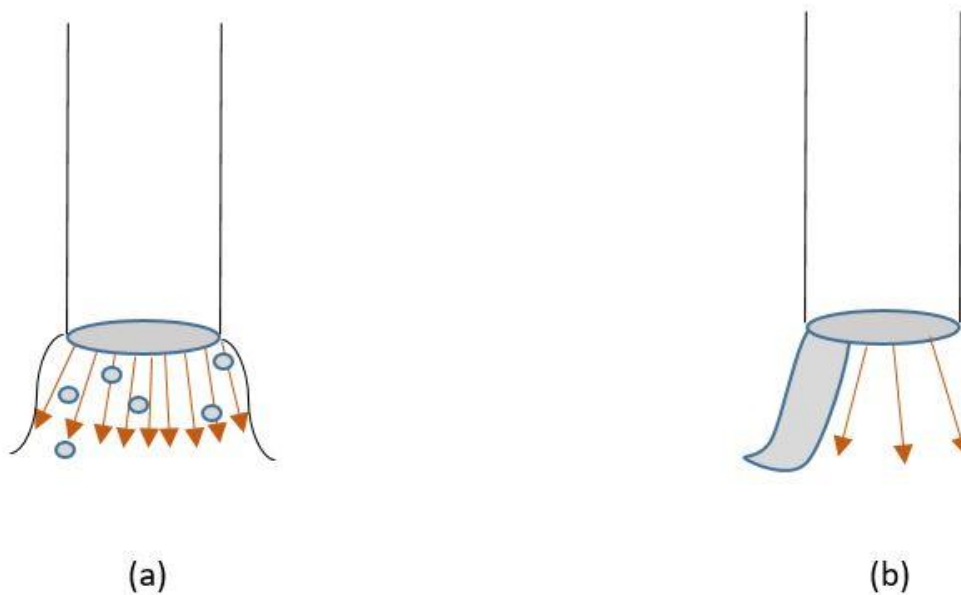


Figure 4-20: Illustration of arc movement at the tip of the electrode E7018 using (a) DC generator, (b) Solid-state power supply.

Analyzing the high-speed videos thoroughly, there is a difference in the detachment as well arc movement between the power supplies, however it is difficult to discern from stills captured in Fig 4-18 and 4-19 due to the rapid movement of the arc attachment point. The outline in each of the high-speed images, approximately mark the flux-wall. The mode of transfer that takes place in the above snapshots is flux-wall guided transfer. However, when DC generator power supply is used, we observe that the arc keeps on bouncing rapidly from side to side, breaking the flux wall and thereby depositing the metal. This is in contrast, when using the Solid-state power supply, the arc movement is very restricted and the metal is deposited through the pre-established flux wall flow. This movement of arc at the tip of the electrode can be illustrated by Fig 4-20 shown above.

Observing the high-speed video and the schematic illustration in Fig 4-20, it can be understood that the frequent bouncing of the arc helps to promote a break-down of the flux wall

and this induces smaller metal droplets. This implies that the arc pressure is more evenly distributed across the electrode, resulting in an easier control of the arc. However, in case of the Solid-state equipment (Fig 4-20b) we observe that the arc does not break the flux wall, rather consistent metal deposition takes place through the established flux wall. This, in turn means that the arc is concentrated at one side of the electrode, resulting in a slightly higher arc pressure as compared to what was observed with DC generator power supply. Figure 4-14 shows the heatscatter plot with the concentrated region. The reason for consistent movement of arc, in case of the DC generator power supply, is the operating range of current, which has a significant amount of variation around the average value, which helps break the flux wall and maintain a slightly more stable arc. However, Fig 4-14b indicates that the reduced current scatter also reduces the movement of the arc and the arc pressure, which results in a higher voltage range because of the higher arc length range.

4.4 Auxiliary Output Comparisons

This section compares a range of other outputs associated with the welding process that are linked to power supply performance: power plots, accelerometer measurements of the welder's hand, electrode melt-off rate, arc force control, an joint gap bridging ability, and bead appearance. Power plots are the term given to a graph between average power and root-mean-squared (RMS) power. The ratio of RMS to average power is known as form factor, and this is a characteristic of the power supply. However, as seen from the power plot shown in figure 4-21, the results from various experiments fall within that 95% CI of the 1:1 line regardless of the power supply.

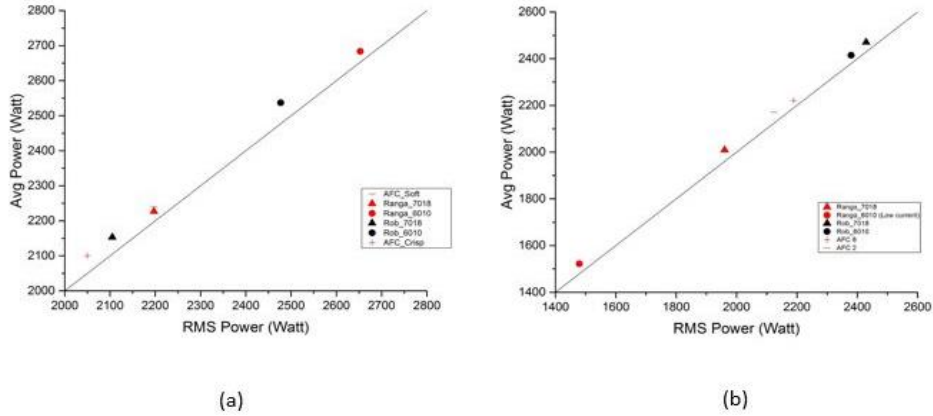


Figure 4-21: Power plot using (a) DC generator power supply, (b) Solid-state power supply.

One of the key inputs of the welder is the electrode position, and this is adjusted more based on the observed response of the arc. An accelerometer (based on a smartphone sensor) was used to measure these inputs during welding in order to determine if these user inputs differed notably for the two power supplies. The accelerometer test measures the acceleration in the axis perpendicular to the workpiece/ plate, and this value along with its derivative versus time are given in Fig 4-22 and 4-23 respectively.

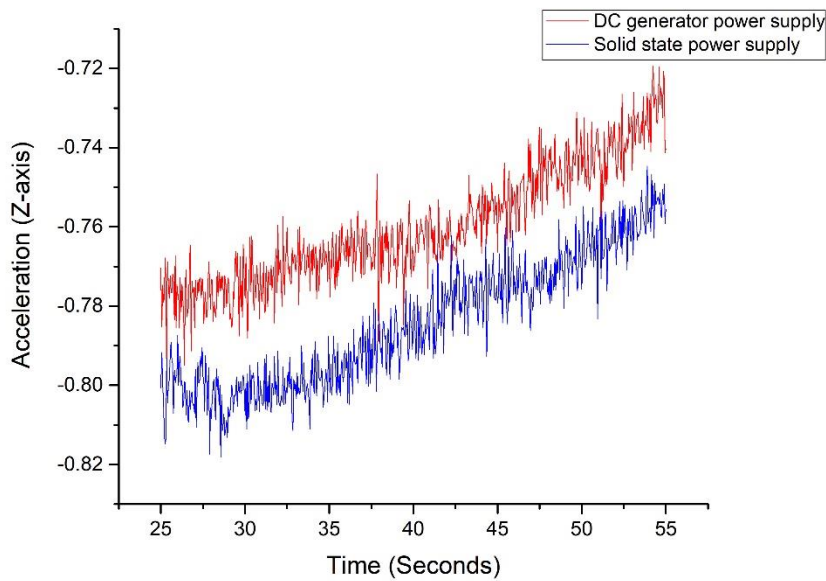


Figure 4-22: Plot of acceleration vs time for both power supplies.

The measurement of acceleration and calculating the derivative of acceleration gives information about the arc pressure, as very high acceleration derivative would mean higher arc pressure and vice versa. The inclination observed in the acceleration graph is due to the consumption of electrode. However, observing Fig 4-22 and 4-23 above, it can be concluded that there was no clear difference in the welder movements due to the arc behaviour.

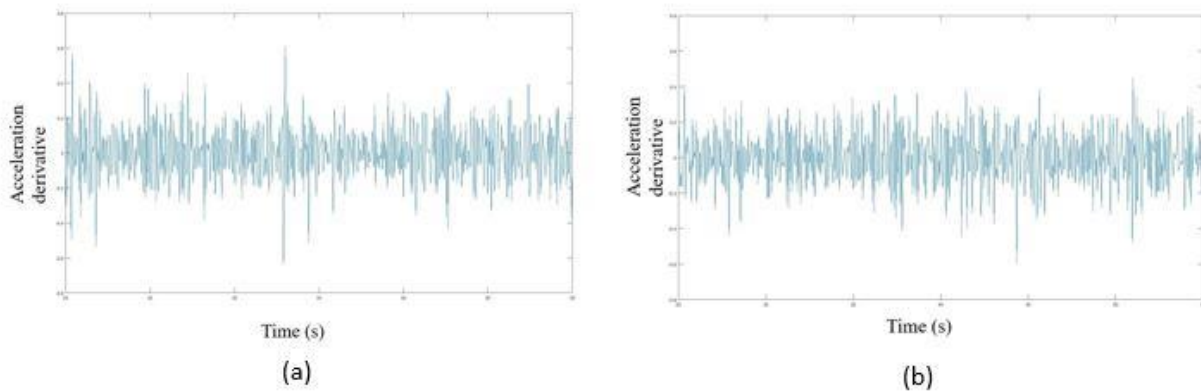
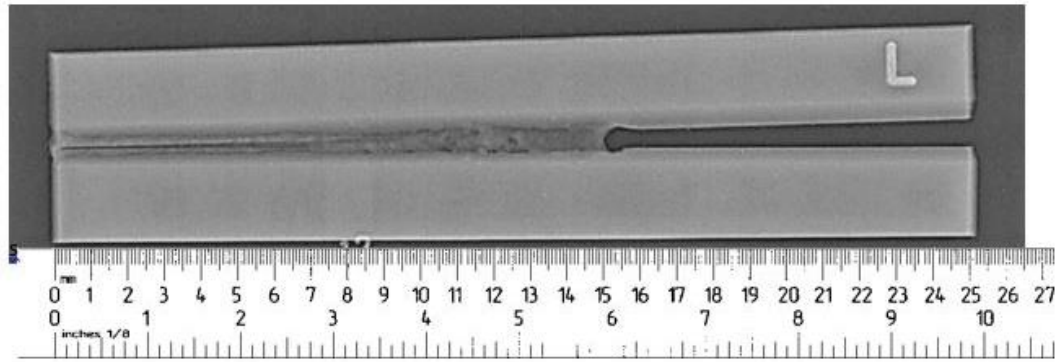
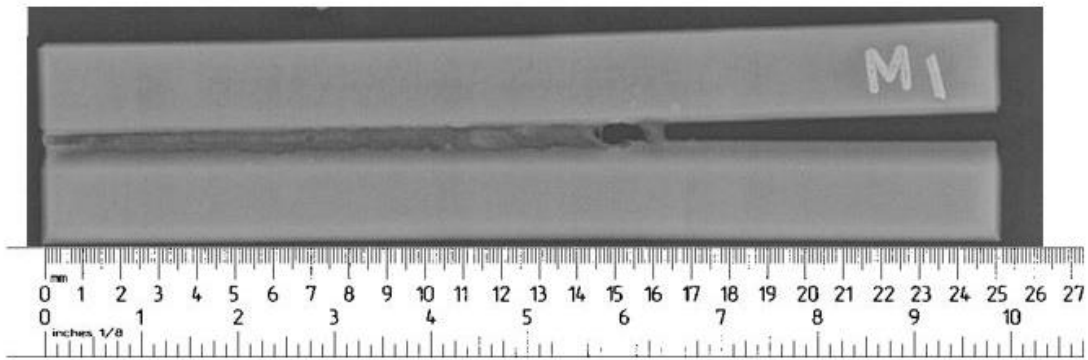


Figure 4-23: Plot of acceleration derivative vs time using (a) DC generator, (b) Solid-state.

In order to compare the flexibility with which the operator can weld, joints were prepared with an increasing gap (using a shim at one side) as specified in Chapter 3. The welder attempted to keep welding until it became difficult to deposit metal because of excessive gap between the plates. With both power supplies, the length that could be welded was around 15 cm based on visual inspection, corresponding to a maximum gap of 3 mm. However, there could be lack of penetration or defects present before the 15 cm distance. Therefore, radiography was performed on both samples, and Fig 4-24 shows the x-rays of the increasing gap tests. No defects were observed in the totality of welding length and it can be concluded that regardless of choice of power supply, the flexibility to weld increasing gap size remains similar for that particular operator, likely due to their ability to adjust their technique to compensate for the gap.



(a)



(b)

Figure 4-24: X-Ray of samples of increasing gap welded using (a) DC generator power supply (b) Solid-state power supply.

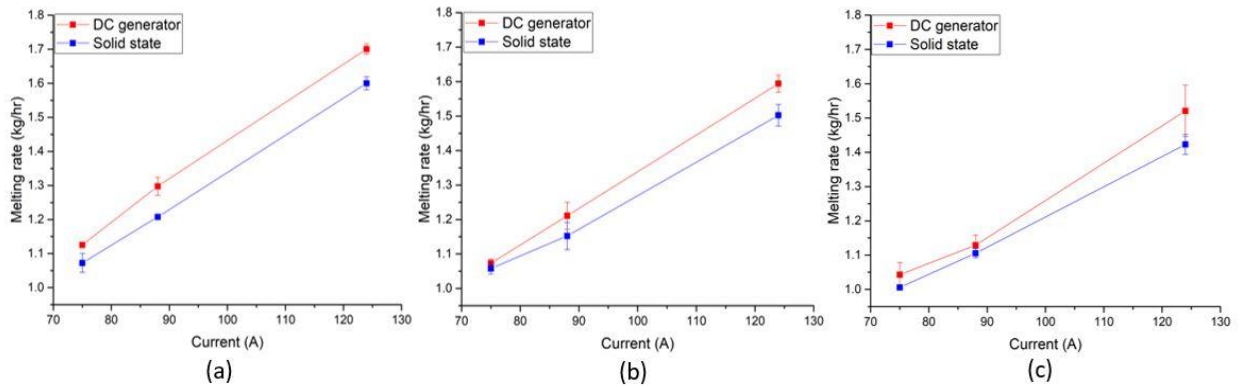


Figure 4-25: Comparison of melting rates of E6010 between power supplies; operator (a) Experienced, (b) Intermediate, (c) Novice.

Another important test is the comparison of melt-off rates of E6010 and E7018 between the two power supplies. The welding was performed with each electrode and each power supply by three different operators: Novice, Intermediate and the Expert welders. Figures 4-25 and 4-26

shows the comparison plot (with error bars) of melting rates for the electrode E6010 and E7018 respectively. The general trend observed from the two plots is that the melting rate of the electrode when the operator is experienced is greater than the melting rate of the electrode when the operator is intermediate or novice, as can be expected. Even though the average current level recorded was the same for both power sources, at a particular current, the melt-off rate generated by the DC generator power supply is greater than that obtained with the Solid-state power supply. This can be explained by two reasons: first, by the current waveform generated by the power supply in response to a short circuit event as shown in Fig 4-3. It was already noted that there is a gradual increase in the current to its peak and a gradual fall of current after the short circuit using the DC generator equipment. Since, the arc is re-established when the current reaches its peak, this means when the current is gradually reduced back to its average level, there is a rise in voltage. This leads to a higher melt-off rate during short circuit events. During the flux-wall guided metal transfer when there is no short circuit, the background current level around is responsible for the higher melt-off rate observed with DC generator power supply as seen from Fig 4-14.

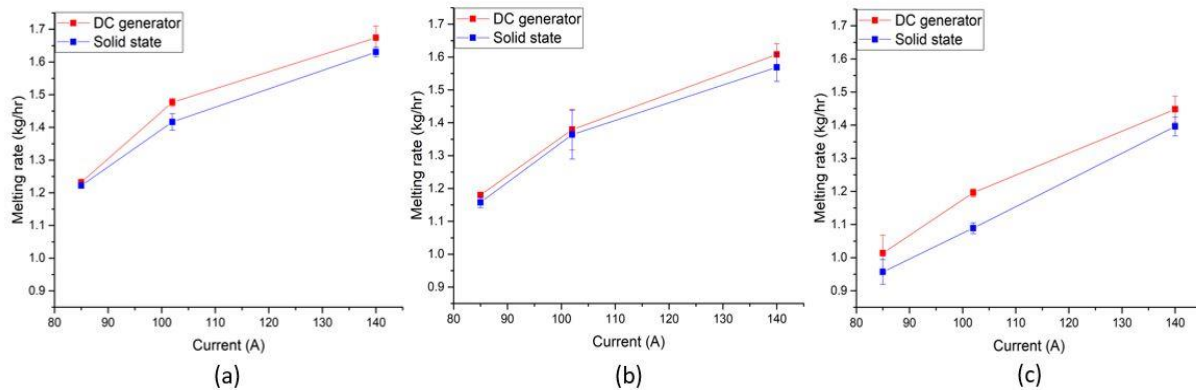


Figure 4-26: Comparison of melting rates of E7018 between power supplies; operator (a) Experienced, (b) Intermediate, (c) Novice.

This difference in productivity could add to the labor costs, which is related to the deposition rate as shown in the equation below. The operator factor is the percentage of time that the welder is actually welding, as a large amount of time is spent in set-ups, slag removal and changing of electrodes. Labor costs are generally calculated using the formula given below. Consider an example, where the welder is working for 2000 hours an year, with an operator factor of, say 10%. This means, he spends 200 hours in welding. Consider the current value to be set at 102 A, at which level the power supplies produce a difference of 0.1 kg/hr in deposition rate. This in turn, means that with DC generator power supply, the welder would be able to deposit 20 kg weld metal more than the amount that could be deposited with Solid-state power supply. In order to match this difference, the welder has to work an extra 20 hours, which will result in an excess of labor cost of around \$2000, given that average labor rate is \$100/hr. Therefore, depending on the labor rate and operator factor, the difference in labor costs could vary between \$2000 and \$5000 per year.

$$\text{Labor costs} = \frac{(\text{Labor} + \text{overhead costs/hr}) * (\text{amount of weld deposited/weld})}{\text{Deposition rate} * \text{Operator factor}}$$

The previous paragraph compares the melt-off rate generated by the two power supplies. If the average current level is the same, then the heat input will be the same for both the machines and hence the mechanical properties are expected to be similar for the joint. However, with the goal of achieving similar mechanical properties, the average current level should be the same for both the machines. Since, pipeline welders can often have a small range of choice for the current input based on the electrode and welding procedure specification this can lead to minor differences in cooling rate and the steel properties. In the present tests, the pipeline welder who replicated the pipeline experiments preferred a slightly higher current with the solid-state power supply, in order

to achieve the same productivity. This leads to a difference in bead appearance, and/or mechanical properties. The bead appearance for welds performed in 45° downhill position with both the power supplies is shown in Fig 4-27. It can be seen that, since the heat input was higher on the right hand side, the height of the weld bead is greater than what is observed with the DC generator power supply. It can be stated that the DC generator power supply produces a batch-wise deposition while the Solid-state provides a more continuous and smooth deposition. The batch-wise deposition is a result of rapid arc movement at the tip of electrode, thereby breaking the flux wall into smaller droplets, while the continuous and smooth deposition is a result of the continuous flow of metal through an already established flux wall that is broken less frequently.



Figure 4-27: Bead appearance for welds performed at 45° downhill position by an experienced pipeline welder using (a) DC generator power supply, (b) Solid-state power supply.

One other output deals with arc force control (AFC) and the effect AFC has on the heatscatter plots when using the Solid-state equipment. The arc force control, as described in the literature review, is the amount of so-called ‘dig’ character offered by the machine, which controls the peak current level during short circuit when there is a surge in the current. Figure 4-28 shows the difference between a low arc force and a high arc force control setting.

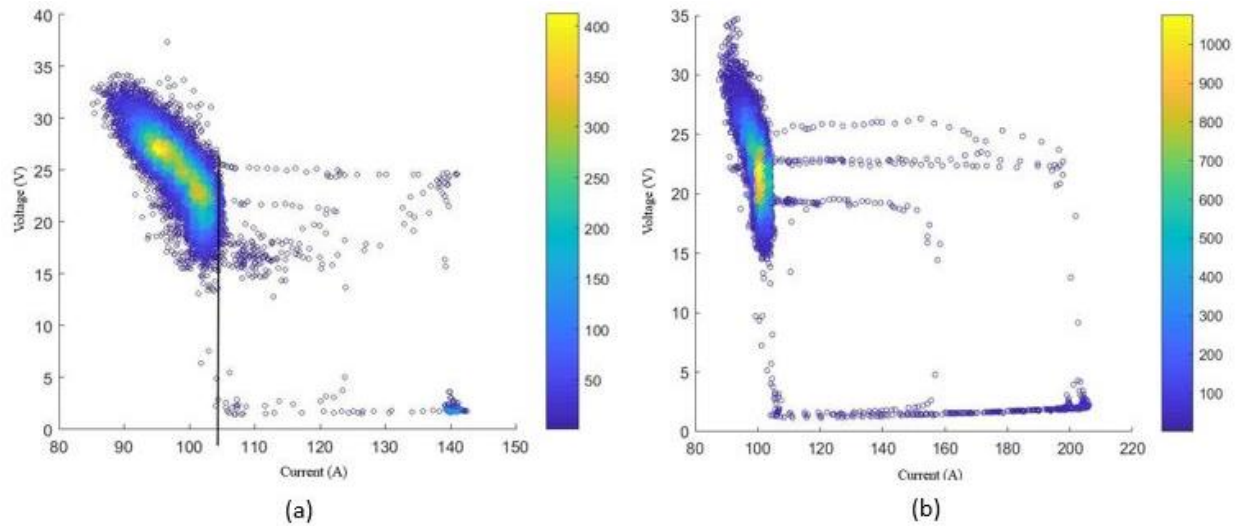


Figure 4-28: Heatscatter plots generated from voltage and current signals recorded when using Solid-state power supply with (a) Low AFC, (b) High AFC.

In the plot in Fig 4-28, the arc force is low on the left side and is high on the right side. It can be seen from the plot, where the peak current during short circuit is different for the two plots. A lower AFC implies, smaller amount of dig, and therefore, the current peak during short circuit is lower (around 140 A) to what is observed with a higher AFC (around 210 A). The results comparing the performance here provide a basis for determining how the design influences the V/I behavior, and how the variation in current levels account for melt-off rate as well as a stable arc. The lower AFC setting achieves this to some extent, with the current range being increased on the lower side of the pre-set current level providing a sharp cut-off point at the average value of current.

4.5 Explanations for the reasons provided for the preference

The primary reason provided by the pipeline welders was the relatively tighter arc provided by DC generator power supply as compared to solid state power supply. Fig 4-14 shows the heatscatter plot with the concentrated regions marked by the ellipse that comprises 65% of the scatter points, which in turn provides us the operating range of current and voltage supplied by the

machine. As can be seen from the figure, DC generator power supply provides a lower voltage range in comparison to that of solid-state power supply. This explains the tighter arc provided by DC generator power supply.

Analyzing the high speed videos with the 515 nm filter pointed out the key difference in the metal transfer of E7018 between the two power supplies. Fig 4-20 shows the movement of the arc at the tip of the electrode 7018. It can be understood after analyzing the videos and the illustration that the frequent bouncing of the arc helps break down the flux wall into smaller droplets. Another difference from the heatscatter plot in Fig 4-14 is the current operating range where DC generator power supply provides around 35 A and solid-state power supply provides around 21 A. The frequent bouncing of the arc explains the easy restart-ability provided by DC generator power supply as frequent arc movement at the tip helps to break the arc. Even though SMAW requires a CC power source, DC generator power supply allows for much variation in the current operating range. However, solid-state power supply trying to restrict the current within a particular range makes it difficult for the welder to work with. Thus DC generator power supply's wider current range accounts for the easier control of the arc provided by the power supply.

Chapter 5

Concluding remarks and recommendations for future work

5.1 Conclusions

Metal transfer phenomenon in the Shielded metal arc welding process was explained by synchronizing high-speed videos with the current and voltage signals recorded with the high-speed DAQ system. The droplet formation and mode of metal transfer was compared between to the two power supplies.

Welding experiments were carried out with different operators, electrodes and welding positions in order to cancel out their influence and try to find how the characteristics of power supply alone affect the current and voltage signals. The power supplies generated their unique current pulse profile. DC generator power supply produced a current waveform that had a triangular shaped waveform with gradual rise and fall in current during short circuit events. On the other hand, Solid-state power supply produced a near square current waveform with rapid increase and fall in the current.

Heat scatter plots were generated using Matlab. These heatscatter plots are scatter plots of voltage vs current with the intensity scale showing the amount of points in the vicinity of a particular point. The heatscatter plots obtained from the experiments that replicated pipeline welding were analyzed and the concentrated regions that were affected by the characteristics of power supply were marked. It was noted that the current range that was allowed by DC generator power supply was 35 A, which was greater than what Solid-state power supply allowed (21A). On the other hand, the voltage range allowed by DC generator power supply was 13 V compared to

18 V range allowed by Solid-state power supply. This explained the tighter arc produced by the DC generator power supply. In order to find out, how these concentrated regions affect the metal transfer, melt-off rates etc., high-speed imaging and some other additional tests were performed.

Analyzing the high speed videos, the predominant mode of metal transfer in E6010 was identified to be short circuit transfer while the predominant mode of transfer observed in E7018 was flux wall guided metal transfer. With the 900 nm wavelength narrow band pass filter, it was difficult to find if there were any differences in the metal transfer between the two power supplies. However, the 515 nm filter pointed out the difference in the metal transfer of E7018 between the power supplies. The arc movement at the tip of the electrode resulted in how the material was transferred, with the arc bouncing rapidly with the DC generator power supply, while less rapid arc movement was observed with Solid-state power supply. Relating it to the heatscatter plot, it was concluded that the higher current range offered by DC generator power supply was responsible for the rapid arc movement and thus producing more stable arc with even arc pressure at the tip of the electrode, thereby making it easier for the welder.

Finally, calculation of melt-off rates for the electrodes with both power supplies was carried out. It was found that, for the same average current level, DC generator power supply offered better melt-off rates as compared to Solid-state power supply in case of both the electrodes E6010 and E7018. Since short circuit/ explosive transfer were observed in E6010, it was concluded that better melt-off rate was obtained with DC generator power supply because of its gradual fall in current after the re-establishment of the arc. This meant a relatively higher average current during the transfer resulting in a better melt-off rate. However, in the case of E7018 where flux-wall guided transfer was observed, the reason for better melt-off rate with DC generator power supply was because of the fact that the background current variation is more in DC generator as

compared to Solid-state. Therefore, with the same current input for the two power supplies, the productivity with DC generator power supply is more than what is offered by Solid-state power supply. This in turn means that the welder becomes fatigue sooner with Solid-state power supply for two reason, one being lower melt-off rate (more time to finish the welding job) and secondly, because of the uneven arc pressure generated at the tip of the electrode by the power supply.

5.2 Recommendations for future work

The first step in incorporating the design of DC generator power supply in Solid-state power supply can be employed by lowering the arc force control and repeating the tests to find out how the metal transfer mode has been affected and calculate melting rates to find if the Solid-state power supply offers the same melt-off rate as DC generator, if not better.

An alternative option would be to add inductance to the circuit of the Solid-state power supply and try to find if the smoothing of the current rise and fall has contributed to change in metal transfer phenomenon observed and melt-off rate measurements.

Calorimetry tests can be performed to measure the actual heat input supplied by the power supply and compare the heat input, deposition rate and mechanical properties between the power supplies. Calorimetric tests and comparison of mechanical properties offered by the power supplies are necessary to measure the quality outputs as the power supply that offers a lower melt-off rate might produce welds with superior mechanical properties or lower overall heat input.

References

- [1] R. A. Jeshvaghani, E. Harati, M. Shamanian, “Effects of surface alloying on microstructure and wear behavior of ductile iron surface-modified with a nickel-based alloy using shielded metal arc welding”, *Materials and Design*, vol. 32, 2011, pp. 1531-1536
- [2] K. Weman, “Welding Processes Handbook”, 2012, 2nd Edition.
- [3] V. Goel, T. W. Liao, K. S. Lee, “A shielded metal arc welding expert system”, *Computers in Industry*, vol. 21, issue 2, 1993, pp. 121-129, ISSN 0166-3615.
- [4] Hobart Institute of Welding Technology, “Shielded Metal Arc Welding”, 2012.
- [5] The Japan Welding Society, “Power generators for arc welding”, *Welding Technique*, vol. 35, 1987, pp. 78-85.
- [6] IM 10292-A “Operator’s Manual- Classic 300MP”, *DC generator Electric*, July 2016. Accessed on: September 2018. [Online], Available: https://www.DCgeneratorelectric.com/assets/servicenavigator-public/DC_generator3/im10292.pdf
- [7] OM-262 506E, “Owner’s Manual- Big Blue 350 And 350X PipePro Series”, *Solid-state*, March 2015. Accessed on: September 2018. [Online], Available: https://www.solid-statewelds.com/files/owners-manuals/o262506e_mil.pdf
- [8] Discussion with DC generator Electric Company, 2016.
- [9] C. E. Jackson, “Fluxes and Slags in Welding.”, *Weld Res. Bull.*, No. 190, Welding Research Council, New York, NY, 1973
- [10] M. Sidorov, “Founder of welding metallurgy”, *Metallurgist*, vol. 23, issue 10, 1979, pp. 733-736

- [11] N. Benardos, S. Olszewski, “Process of and apparatus for working metals by the direct application of the electric current”, US 363320, patented 17 May 1887
- [12] C. L. Coffin, “Process of welding metals electrically”, US 428459A, patented 20 May 1890
- [13] H. B. Cary, S. Helzer, “Modern Welding Technology”, 2005, Pearson, 6th Edition.
- [14] K. Sindo, “Welding Metallurgy Second Edition”, Hoboken, NJ: John Wiley & Sons, 2003.
- [15] P. Smith, “Joints for process piping systems”, *Piping Materials Guide*, Gulf Professional Publishing, 2005, pp. 171-199, ISBN 9780750677431
- [16] DC generator Electric, “Constant current vs. constant voltage output”, 2018 [Online]. Available: <https://www.DCgeneratorelectric.com/en-ca/support/process-and-theory/Pages/constant-current-vs-constant-voltage-output.aspx>
- [17] M. F. Hoyaux, “Arc Physics.”, *Springer*, Verlag New York Inc., 1968
- [18] Solid-state, “Selecting a Constant Current (CC) DC Welder for Training Purposes”, 2018 [online]. Available: <https://www.solid-statewelds.com/resources/article-library/selecting-a-constant-current-cc-dc-welder-for-training-purposes>
- [19] AWS A5.1/A5.1M:2012, “Specification for Carbon Steel Electrodes for Shielded Metal Arc Welding”, *American Welding Society*, April 10, 2012, [Online], Available: https://pubs.aws.org/Download_PDFS/A5.1-A5.1M-2012PV.pdf
- [20] Kin-Ling Sham, “Flux system design and optimization of shielded metal arc welding for high nickel alloys” MSc. Thesis, Colorado School of Mines, 2009
- [21] Xu, X., "Study of Metal Transfer Modes in Shielded Metal Arc Welding." MSc. M.S. Thesis, Colorado School of Mines, 1994

- [22] V. Kumar, S. K. Albert, N. Chandrasekhar, "Signal processing approach on weld data for evaluation of arc welding electrodes using probability density distributions", *Measurement*, vol. 133, 2019, pp. 23-32, ISSN 0263-2241
- [23] American Welding Society. 1976. *Welding handbook: 7th edition*, vol. 1. Miami, Florida.
- [24] V. Kumar, N. Chandrasekhar, S. K. Albert, J. Jayapandian, "Analysis of arc welding process using Digital Storage Oscilloscope", *Measurement*, vol. 81, 2016, pp. 1-12, ISSN 0263-2241
- [25] "Dynamo", 2018, [online] Available: <https://en.wikipedia.org/wiki/Dynamo>
- [26] T. E. Kooken, "Arc welding power supply", US 5991169, patented 23 November 1999
- [27] B. J. Vogel, "Welding power supply with digital controller", US9492880B2, patented 03 June 2009
- [28] DC generator Electric, "Inverters and Choppers- power electronics technology", 2018, Online. Available: <https://www.DCgeneratorelectric.com/assets/us/en/literature/nx130.pdf>
- [29] E. B. F. Dos Santos, "Influence of current pulse profile on metal transfer in pulsed gas metal arc welding", MAsc. Thesis, University of Waterloo, 2017
- [30] TWI Global, "Power Source Characteristics", 2018, [online], Available: <https://www.twi-global.com/technical-knowledge/job-knowledge/power-source-characteristics-121/>

Appendix A

The heatscatter plot mentioned in Chapter 4 was generated with the MATLAB program shown below.

```
function outfile = heatscatter(X, Y, outpath, outname, numbins,
markersize, marker, plot_colorbar, plot_lsf, xlab, ylab, title)
%%%%%%%%%%%%%%%%%%%%%%%%%%%%%%%%%%%%%%%%%%%%%%%%%%%%%%%%%%%%%%%%%%%%%%%%
%%%%%%%%%%%%%%%%%%%%%%%%%%%%%%%%%%%%%%%%%%%%%%%%%%%%%%%%%%%%%%%%%%%%%%%%

% heatscatter(X, Y, outpath, outname, numbins, markersize,
marker, plot_colorbar, plot_lsf, xlab, ylab, title)

% mandatory:

%X          [x,1] array containing variable X
%Y          [y,1] array containing variable Y

%outpath    path where the output-file should be saved.
%           leave blank for current working directory

%outname    name of the output-file. if outname contains
%           (e.g. png), this type will be used.
%           Otherwise, a pdf-file will be generated

% optional:

%numbins    [double], default 50
%           number of bins used for the
%           heat3-calculation, thus the coloring

%markersize [double], default 10
%           size of the marker used in the scatter-plot

%marker     [char], default 'o'
%           type of the marker used in the scatter-plot

%plot_colorbar [double], boolean 0/1, default 1
%           set whether the colorbar should be plotted
%           or not

%plot_lsf    [double], boolean 0/1, default 1
%           set whether the least-square-fit line
%           should be plotted or not (together with
%           the correlation/p-value of the data
```

```

%xlabel          [char], default ''
%               lable for the x-axis

%ylabel          [char], default ''
%               lable for the y-axis

%title           [char], default ''
%               title of the figure

%%%%%%%%%%%%%%%%%%%%%%%%%%%%%%%%%%%%%%%%%%%%%%%%%%%%%%%%%%%%%%%%%%%%%%%%
%%%%%%%%%%%%%%%%%%%%%%%%%%%%%%%%%%%%%%%%%%%%%%%%%%%%%%%%%%%%%%%%%%%%%%%%

%%% mandatory

if ~exist('X','var') || isempty(X)
    error('Param X is mandatory! --> EXIT!');
end
if ~exist('Y','var') || isempty(Y)
    error('Param Y is mandatory! --> EXIT!');
end
if ~exist('outpath','var')
    error('Param outpath is mandatory! --> EXIT!');
end
if ~exist('outname','var') || isempty(outname)
    error('Param outname is mandatory! --> EXIT!');
end

%%% optional

if ~exist('numbins','var') || isempty(numbins)
    numbins = 50;
else
    % force number, not char input
    numbins = str2double(numbins);
end
if ~exist('markersize','var') || isempty(markersize)
    markersize = 10;
else
    % force number, not char input
    markersize = str2double(markersize);
end
if ~exist('marker','var') || isempty(marker)
    marker = 'o';
end
if ~exist('plot_colorbar','var') || isempty(plot_colorbar)
    plot_colorbar = 1;
end
if ~exist('plot_lsf','var') || isempty(plot_lsf)
    plot_lsf = 1;
end
end

```

```

if ~exist('xlab','var') || isempty(xlab)
    xlab = '';
end
if ~exist('ylab','var') || isempty(ylab)
    ylab = '';
end
if ~exist('title','var') || isempty(title)
    title = '';
end

[values, centers] = hist3([X Y], [numbins numbins]);
centers_X = centers{1,1};
centers_Y = centers{1,2};
binsize_X = abs(centers_X(2) - centers_X(1)) / 2;
binsize_Y = abs(centers_Y(2) - centers_Y(1)) / 2;
bins_X = zeros(numbins, 2);
bins_Y = zeros(numbins, 2);
for i = 1:numbins
    bins_X(i, 1) = centers_X(i) - binsize_X;
    bins_X(i, 2) = centers_X(i) + binsize_X;
    bins_Y(i, 1) = centers_Y(i) - binsize_Y;
    bins_Y(i, 2) = centers_Y(i) + binsize_Y;
end

scatter_COL = zeros(length(X), 1);
onepercent = round(length(X) / 100);
fprintf('Generating colormap...\n');
for i = 1:length(X)
    if (mod(i,onepercent) == 0)
        fprintf('.');
    end

    last_lower_X = NaN;
    last_higher_X = NaN;
    id_X = NaN;
    c_X = X(i);
    last_lower_X = find(c_X >= bins_X(:,1));
    if (~isempty(last_lower_X))
        last_lower_X = last_lower_X(end);
    else
        last_higher_X = find(c_X <= bins_X(:,2));
        if (~isempty(last_higher_X))
            last_higher_X = last_higher_X(1);
        end
    end
end
if (~isnan(last_lower_X))
    id_X = last_lower_X;
end

```

```

else
    if (~isnan(last_higher_X))
        id_X = last_higher_X;
    end
end

last_lower_Y = NaN;
last_higher_Y = NaN;
id_Y = NaN;

c_Y = Y(i);
last_lower_Y = find(c_Y >= bins_Y(:,1));
if (~isempty(last_lower_Y))
    last_lower_Y = last_lower_Y(end);
else
    last_higher_Y = find(c_Y <= bins_Y(:,2));
    if (~isempty(last_higher_Y))
        last_higher_Y = last_higher_Y(1);
    end
end
if (~isnan(last_lower_Y))
    id_Y = last_lower_Y;
else
    if (~isnan(last_higher_Y))
        id_Y = last_higher_Y;
    end
end

scatter_COL(i) = values(id_X, id_Y);
end

fprintf(' Done!\n');
fprintf('Plotting...');

f = figure();
scatter(X, Y, markersize, scatter_COL, marker);

if (plot_colorbar)
    colorbar;
end
%{
if (plot_lsf)
    [r,p] = corr(X, Y);
    str = {sprintf('corr: %.3f', r), sprintf('pval: %d',
p)}};
    l = lsline;
    set(l, 'Color', 'k');
    annotation('textbox', [0.14 0.80 0.1 0.1], 'String',
str, 'EdgeColor', 'none');

```



```
    end
    %}
    if (~isempty(xlab))
        xlabel(xlab);
    end
    if (~isempty(ylab))
        ylabel(ylab);
    end
    if (~isempty(title))
        title(title);
    end

    [p,n,r] = fileparts(outname);
    if (isempty(r))
        r = '.pdf';
    end
    outname = strcat(p,n,r);
    outfile = fullfile(outpath, outname);
    saveas(f, outfile);
    fprintf(' Done!\n');
end
```